JHU/APL
TG 1364
JULY 1985

AD-A191 306

FINAL

Technical Memorandum

STRUCTURAL ALTERATIONS IN THE CORNEA FROM EXPOSURE TO INFRARED RADIATION

R. A. FARRELL
R. L. McCALLY
C. B. BARGERON
W. R. GREEN

81MM1504

DTIC
SELECTED
FEB 2 3 1988
E

THE JOHNS HOPKINS UNIVERSITY ■ APPLIED PHYSICS LABORATORY

88 2 22 192

REPORT DOCUMENTATION PAGE

1a. REPORT SECURITY CLASSIFICATION	1b. RESTRICTIVE MARKINGS
Unclassified	–

2a. SECURITY CLASSIFICATION AUTHORITY	3. DISTRIBUTION/AVAILABILITY OF REPORT
–	Approved for public release; distribution unlimited.
2b. DECLASSIFICATION/DOWNGRADING SCHEDULE	
–	

4. PERFORMING ORGANIZATION NUMBER(S)	5. MONITORING ORGANIZATION REPORT NUMBER(S)
JHU/APL TG 1364	JHU/APL TG 1364

6a. NAME OF PERFORMING ORGANIZATION	6b. OFFICE SYMBOL (If Applicable)	7a. NAME OF MONITORING ORGANIZATION
The Johns Hopkins University Applied Physics Laboratory	TIR	Letterman Army Institute of Research

6c. ADDRESS (City, State, and ZIP Code)	7b. ADDRESS (City, State, and ZIP Code)
Johns Hopkins Road Laurel, Maryland 20707	Presidio of San Francisco, CA 94129-6815

8a. NAME OF FUNDING/SPONSORING ORGANIZATION	8b. OFFICE SYMBOL (If Applicable)	9. PROCUREMENT INSTRUMENT IDENTIFICATION NUMBER
U.S. Army Medical Research and Development Command		N00039-87-C-5301

8c. ADDRESS (City, State, and ZIP Code)	10. SOURCE OF FUNDING NUMBERS			
	PROGRAM ELEMENT NO.	PROJECT NO.	TASK NO.	WORK UNIT ACCESSION NO.
Fort Detrick Frederick, Maryland 21701- 5012			ZP20	

11. TITLE (Include Security Classification)

Structural Alterations in the Cornea from Exposure to Infrared Radiation

12. PERSONAL AUTHOR(S)

R. A. Farrell, R. L. McCally, C. B. Bargeron, and W. R. Green

13a. TYPE OF REPORT Final Technical Memorandum	13b. TIME COVERED FROM 7/1/77 TO 6/30/85	14. DATE OF REPORT (Year, Month, Day) 1985, July	15. PAGE COUNT 41

16. SUPPLEMENTARY NOTATION

This report covers MIPRs 7951, 0029, 8952, and 81MM1504.

17. COSATI CODES			18. SUBJECT TERMS
FIELD	GROUP	SUB-GROUP	CO_2 laser damage endothelial damage thermal damage models
			corneal damage stromal damage single-pulse exposures
			epithelial damage wound healing multiple-pulse exposures

19. ABSTRACT (Continue on reverse if necessary and identify by block number)

This report summarizes our research on the interaction of infrared radiation, especially from CO_2 lasers, with the cornea. The research reported here was carried out between July 1, 1977 and June 30, 1985. The report discusses laser systems, animals, endothelial temperature histories, endothelial damage thresholds, stromal damage, wound repair, epithelial damage from single- and multiple-pulse exposures, and a new thermal damage model based on a phase transition. Keywords: exposure (physiology); Laser damage; Laser hazards; physiological effects

20. DISTRIBUTION/AVAILABILITY OF ABSTRACT	21. ABSTRACT SECURITY CLASSIFICATION
☒ UNCLASSIFIED/UNLIMITED ☐ SAME AS RPT. ☐ DTIC USERS	Unclassified

22a. NAME OF RESPONSIBLE INDIVIDUAL	22b. TELEPHONE (Include Area Code)	22c. OFFICE SYMBOL
NAVPRO Security Officer	(301) 953-5403	SE

DD FORM 1473, 84 MAR

JHU/APL
TG 1364
JULY 1985

FINAL

Technical Memorandum

STRUCTURAL ALTERATIONS IN THE CORNEA FROM EXPOSURE TO INFRARED RADIATION

R. A. FARRELL
R. L. McCALLY
C. B. BARGERON
W. R. GREEN

81MM1504

THE JOHNS HOPKINS UNIVERSITY ■ APPLIED PHYSICS LABORATORY
Johns Hopkins Road, Laurel, Maryland 20707

ABSTRACT

This report summarizes our research on the interaction of infrared radiation, especially from CO_2 lasers, with the cornea. The research reported here was carried out between July 1, 1977 and June 30, 1985. The report discusses laser systems, animals, endothelial temperature histories, endothelial damage thresholds, stromal damage, wound repair, epithelial damage from single- and multiple-pulse exposures, and a new thermal damage model based on a phase transition.

SUMMARY

This report summarizes our research on the interaction of infrared radiation, especially from CO_2 lasers, with the cornea. The research reported here was conducted between July 1, 1977 and June 30, 1985. The following topics are addressed:

- Laser systems,
- Animals,
- Endothelial temperature histories,
- Endothelial damage thresholds,
- Stromal damage,
- Wound repair,
- Epithelial damage from single- and multiple-pulse exposures, and
- Thermal damage model.

Sections 1.0 and 2.0 contain general descriptions of the laser systems, methods of beam characterization, and animal care and handling methods used throughout the reporting period. More specialized experimental details are presented as necessary in the appropriate sections.

In Section 3.0 we report calculations of the endothelial temperature caused by exposing the cornea to CO_2 laser radiation. The calculations assume that the laser is operated with a Gaussian beam intensity profile and that the radiation is absorbed according to the Beer-Lambert law. The efficacy of the theoretical model is tested by comparing the calculations with measurements on excised corneas exposed to CO_2 laser radiation. Both a liquid crystal technique and a thermocouple were used to measure the temporal and spatial variations of endothelial temperature. The experimental and theoretical values are in reasonable accord, which gives added confidence in the theoretical model, especially as it could be applied to other laser systems or exposure conditions.

Section 4.0 reports our determinations of endothelial damage thresholds in rabbit corneas for exposure to CO_2 laser radiation. Endothelial damage was detected using a staining technique. Threshold damage is characterized by distorted cells and uneven staining of the cell borders, while at exposure times of up to 90% of the threshold, the stained endothelia were indistinguishable from those in control eyes. Three peak irradiance levels (24.5, 10.0, and 2.6 W/cm^2) were investigated and the exposure duration was varied until threshold damage occurred. In each instance the duration of the threshold exposure for endothelial damage (1.0, 5.2, and 240 s, respectively) was about 10 or more times the accepted duration for threshold epithelial damage. These results suggest that protecting against epithelial damage also will ensure against endothelial damage for CO_2 laser systems. However, the calculated peak temperature increases of the endothelium at its threshold are similar to those of the epithelium at its damage threshold. We show that, either for a larger beam diameter with CO_2 radiation or for other lasers where the absorption length of their radiation is comparable to the corneal thickness, the endothelial temperature rise can approach that of the epithelium for the same exposure. Thus, under these conditions, the endothelial damage threshold could be similar to the epithelial damage threshold.

In Section 5.0 we note that exposures well above the threshold for epithelial damage, but below that for endothelial damage, produce bowl-shaped stromal wounds. In such wounds, light and electron microscopy and slit-lamp photographs all show a sharp demarcation between the damaged and undamaged regions 48 h after exposure. The micrographs also show that the damaged region is acellular. Calculations of the expected temperature increases combined with analyses of slit-lamp photographs show that the wound boundary corresponds to a surface of equal peak temperature increase. Comparisons with epithelial and endothelial damage conditions suggest that stromal, endothelial, and epithelial cells have essentially the same thermal damage mechanism.

In Section 6.0 we discuss the healing process following exposures that produce stromal wounds extending about halfway through the cornea. The lesions were documented by slit-lamp photography and examined by light and electron microscopy. Examinations were carried out at intervals from 1 h postexposure up to 11 months postexposure. The exposures did not damage the epithelial basement membrane. The cornea is covered by a mature and well-adhering epithelium by 1 week. The stromal wounds, which are nearly acellular at 48 h, are repopulated with active fibroblasts by 2 weeks. The wounds are nearly healed by 8 weeks. No inflammatory response or vascularization was observed at any time during the healing period.

In Section 7.0 we present data for damage thresholds of the corneal epithelium resulting from single- and multiple-pulse exposures. To our knowledge, this is the first study of multiple-pulse damage to the cornea. We confirm that damage from single-pulse exposures having durations between 10^{-3} and 10 s can be correlated empirically by a modified critical temperature law in which the critical temperature has a weak dependence on exposure duration. As an additional test of the modified critical temperature model, we also examined the

effect of beam diameter on thresholds for single-pulse exposures. The results supported the modified critical temperature model; i.e., for a fixed exposure duration, the threshold irradiance was that required to produce a fixed peak temperature increase, independent of beam diameter. The damage data for multiple pulses cover exposures from pulse trains of up to 999 pulses, having pulse repetition frequencies between 1 and 100 Hz and individual pulse durations between 10^{-3} and 0.5 s. These data can be correlated empirically either by an approximate critical temperature model, by a model in which the threshold energy density varies approximately as the ¾ power of the number of pulses, or by a model in which the threshold energy density varies approximately as the 0.7 power of the total duration of the pulse train.

In Section 8.0 we introduce a new physical model to explain the weak dependence of the critical temperature on exposure duration that occurs in the empirical modified critical temperature model. We were led to this new model by energy considerations suggesting that threshold damage can be associated with an endothermic phase transition occurring at a fixed temperature. In the model, we associate damage with a fixed amount of energy being supplied to the transition. The new model can correlate all of the single-pulse threshold data. It predicts a transition temperature of 68°C and, if we assume that approximately 5% of the epithelium undergoes the phase change, a latent heat of about 80 cal/g. The analysis suggests that the weak dependence of critical temperature on exposure duration in the empirical model actually is caused by heat conduction away from the damaged region during exposure.

FOREWORD

CONTENTS

ILLUSTRATIONS

TABLES

1.0 LASER SYSTEMS

Two CO_2 lasers were used during the contract period. One was built by us at The Johns Hopkins University Applied Physics Laboratory (APL) in the first year as partial fulfillment of our contract.[1] It was used in all endothelial and stromal experiments and also in many of the epithelial damage threshold experiments for both single- and multiple-pulse exposures. However, the APL-built laser had insufficient power output to produce damage at exposure durations less than 10 ms. We therefore purchased an Apollo Model 517 for the experiments. Both lasers were operated in the TEM_{00} mode for which the beam irradiance follows a Gaussian profile. Laser power levels were measured with a Scientech power meter. The beam irradiance profile was measured at each experimental session with either a $160\text{-}\mu m$ circular aperture or slits having widths of 42 or $16 \mu m$.[2] The $1/e$ radius of the beam is the off-axis distance at which the irradiance in the Gaussian profile is $1/e$ (36.8%) of its value at the center. For a Gaussian beam profile, the peak irradiance, I_0, is related to the total power, P, in the beam by $I_0 = P/A$, where

A is the area within the $1/e$ radius. The nominal $1/e$ beam diameter of the Apollo laser was 4 mm, while that of the laser built at APL was 2.5 mm. In experiments requiring different beam diameters, a zinc selenide lens with a 12.5-cm focal length was inserted into the optical system and the beam profile was determined at the position where the cornea would be located. Damage thresholds are stated as the peak irradiance or peak energy density for the exposure duration under investigation.

Two shutter systems were used to control the exposure durations. A Uniblitz shutter was used for both single- and multiple-pulse experiments in which individual pulse durations were 9 ms or greater. The shutter was operated by a control system that allowed us to set the duration, number, and repetition rate of the pulses. For pulses shorter than 9 ms, a chopper wheel was used in conjunction with the Uniblitz shutter. In this configuration the chopper wheel controlled the individual pulse duration and repetition rate, while the Uniblitz was used as an overall gate to control the number of pulses.

2.0 ANIMALS

New Zealand white rabbits weighing 5 to 7 lb were used for the experiments. During the first several years of our contract we administered sodium pentobarbital (Nembutal®) to anesthetize the animals. In particular, Nembutal® was employed for all endothelial and stromal damage experiments (see Sections 4.0 and 5.0). Subsequently we discovered that a 40:60 mixture of ketamine hydrochloride (100 mg/ml) and xylazine (20 mg/ml) was a more controllable general anesthetic for rabbits and also was better for stopping eye motion—an especially useful feature with longer exposures. The mixture was

used for both the wound healing and the epithelial damage experiments (Sections 6.0 and 7.0). In addition to either of the general anesthesias, proparacaine hydrochloride ophthalmic solution (Alcaine®) was applied topically to the cornea. The anesthetized animals were placed in a conventional holder and were positioned with the aid of a He-Ne alignment laser whose beam was colinear with the CO_2 laser output. The incident radiation was aligned perpendicular to the surface of the cornea. It was sometimes necessary to use a speculum to hold the eye open, particularly for the longer exposures. In such instances the speculum was inserted approximately 1 min before exposure. In all experiments, the cornea was irrigated about 20 s before exposure with a small amount of physiological saline at room temperature. At ~10 s before exposure, excess saline was blotted by holding an absorbent tissue against

[1]C. B. Bargeron, W. R. Green, R. A. Farrell, and R. L. McCally, "Structural Alterations in the Cornea from Exposure to Infrared Radiation," Annual Report to Letterman Army Institute of Research, Presidio of San Francisco, Calif. (Jul 1978).

[2]R. L. McCally, "Measurement of Gaussian Beam Parameters," Appl. Opt. **23**, 2227 (1984).

the limbus just below the area to be exposed. This process assured a reproducible "tear" layer. Because of the small amount of liquid involved, the 10-s interval between blotting and exposure was sufficient to ensure

that the cornea's surface temperature returned to its steady state value. Following exposure, the eye was blinked manually to reform its natural tear film.

3.0 ENDOTHELIAL TEMPERATURE HISTORIES

An understanding of the conditions required for minimal endothelial damage as discussed in Section 4.0 requires knowledge of the temperature-time history of the endothelium following laser exposure. Consequently we developed methods to measure and to calculate the spatial distribution of temperature at the position of the endothelium as a function of time following exposure of the cornea's epithelial surface to CO_2 laser radiation. The calculations assume that the cornea's thermal properties are homogeneous throughout its thickness and, for convenience, are approximated by those of water.[3,4] The measurements use a well-characterized CO_2 laser and serve to test the theoretical model. Once verified in this manner, the model can be used to predict the effects of other laser systems.[5,6]

The calculations are based on a Green's function solution to the heat flow equation for a Gaussian incident beam. The beam is assumed to impinge on a semi-infinite slab and to have a constant peak irradiance for the duration of the exposure. The solution $T(r,z,t)$, where r is the radial distance from the beam axis, z is the depth from the front surface, and t is the time after the initiation of exposure, is given in terms of a definite integral.[1,7] In Ref. 1 we outlined the derivation of this integral, both for the case of total surface absorption and for Beer's law absorption, and gave a listing of the computer program (available on request) that we wrote for its evaluation.

This theoretical model neglects heat loss via convection, radiation, and evaporation from the warm anterior surface. We showed that these losses are insignificant for the exposure conditions encountered in the endothelial damage threshold experiments.[5] (Since these exposures are more severe than those in the stromal damage experiments discussed in Sections 5.0 and 6.0, it follows that such approximations are valid there as well.)

The Green's function solution does not account for the latent heat associated with phase transitions such as tear-film boiling, which could occur in exposures where the anterior surface reaches 100°C, or protein denaturation, which occurs at about 60°C.[4] Although methods are available for including phase transitions in heat flow calculations (see Section 8.0),[7,8] we elected, for the purposes of this section, to use the Green's function approach to obtain an upper bound on the endothelial temperature. One objective of the experimental measurements was to test how well this bound approximates the actual temperature.

Experimental temperatures were obtained with excised corneas using either a thermocouple or a liquid crystal technique.[5] The thermocouple measures temperatures over a wide range, but only at a single position in space. On the other hand, the liquid crystal technique has a limited practical operating range and is less precise, but

[1] \. S. Brownell and B. E. Stuck, "Ocular and Skin Hazards from CO_2 Laser Radiation," in *Proc. 9th Army Science Conf.*, pp. 123-138 (Jun 1974).
[4] D. E. Egbert and E. F. Maher, *Corneal Damage Thresholds for Infrared Laser Exposure: Experimental Data, Model Predictions, and Safety Standards*, U.S.A.F. School of Aerospace Medicine, Brooks AFB, SAM-TR-77-29 (1977).
[5] C. B. Bargeron, R. L. McCally, and R. A. Farrell, "Calculated and Measured Endothelial Temperature Histories of Excised Rabbit Corneas Exposed to Infrared Radiation," *Exp. Eye Res.* **32**, 241-250 (1981).
[6] C. B. Bargeron, R. A. Farrell, W. R. Green, and R. L. McCally, "Corneal Damage from Exposure to Infrared Radiation: Rabbit Endothelial Damage Thresholds," *Health Phys.* **40**, 855-862 (1981).
[7] H. S. Carslaw and J. C. Jaeger, *Conduction of Heat in Solids*, Oxford University Press, Oxford (1959).
[8] S. G. Bankoff, "Heat Conduction or Diffusion with Change of Phase," *Adv. Chem. Eng.* **5**, 51-122 (1964).

measures temperature over the entire endothelial surface.

In the liquid crystal technique, crystals were painted onto thin (25-μm) black mylar disks that were preformed to match the corneal curvature. The disks were attached at their edges to excised corneas using cyanoacrylate cement. The corneas were mounted in an appropriate holder and motion pictures were made of the color changes in the liquid crystals as the cornea responded to the laser exposure. The films were subsequently evaluated as described in Ref. 5 to obtain the temperature-time histories at various radial distances from the laser beam axis.

Representative data obtained using the liquid crystal method are shown in Figs. 1 and 2 for two different exposures, each near the epithelial damage threshold for the corresponding experimental irradiance level. The error bars primarily reflect the difficulty in estimating the color variation of the crystals. Figure 1 shows the spatial variation of the temperature increase and indicates that the temperature rise falls off sharply at the 1/e radius of the beam ($r_{1/e}$ = 1.0 mm). Figure 2 shows the temperature increase on the beam axis and compares it to the calculated value.
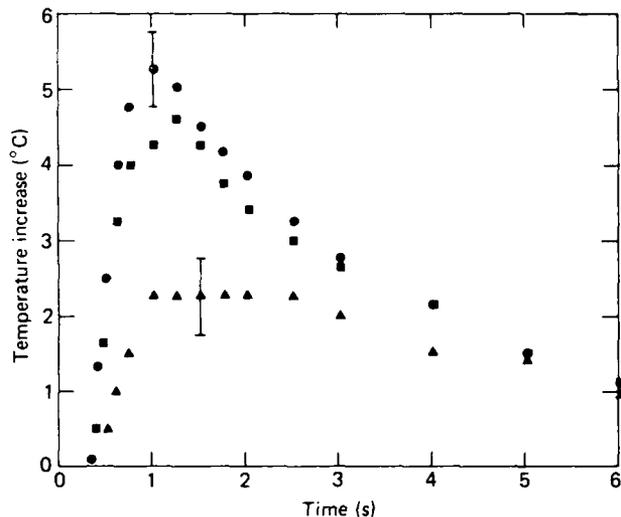
Figure 1 The measured endothelial temperature increase as a function of time at three radial positions from the beam axis. The liquid crystal technique was used for these measurements. The time, t = 0, corresponds to the initiation of exposure. The peak irradiance was 11.0 W/cm^2, the exposure duration was 0.50 s, and the 1/e radius of the beam was 1.0 mm. The circles represent the data on the beam axis (r = 0); the squares represent the data at r = 0.5 mm; and the triangles represent the data at r = 1.0 mm. The error bars indicate an uncertainty of ±0.5°C.
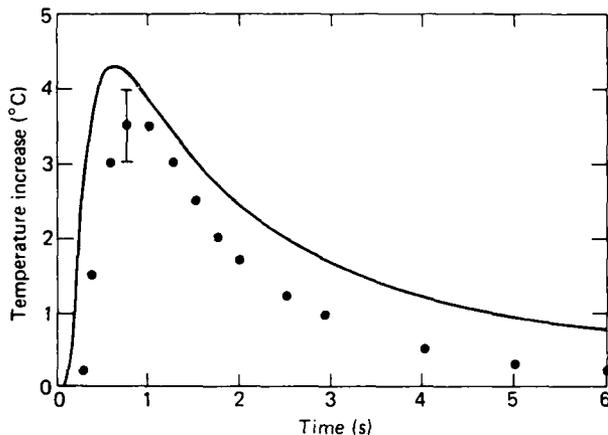
Figure 2 The circles are liquid crystal measurements of the endothelial temperature increase on the beam axis as a function of time. The curve is the calculated value. The peak irradiance was 25.1 W/cm^2, the duration was 0.104 s, and the 1/e radius of the beam was 1.0 mm. For the calculation, the thickness was taken as 0.500 mm to account for the corneal thickness measured at zero transcorneal pressure and the thickness of the plastic film.

The thermocouple temperature measurements were made using a 0.025-mm-diameter chromel-alumel thermocouple. The small thermal inertia associated with this thermocouple gave it a rapid response time, and the conductive heat loss from the junction via the small diameter wires was negligible for our experimental conditions. (Details of constructing and mounting the thermocouple are given in Ref. 5.) The junction was positioned carefully at the endothelial surface of the mounted cornea with the aid of a slit-lamp microscope. Accurate positioning of the probe on the center of the laser beam was accomplished by moving the cornea holder/thermocouple assembly with an x-y micropositioner until we obtained the maximum temperature rise for a very low exposure (i.e., 25 W/cm^2 for 0.05 s, which is well below the epithelial damage threshold). This method ensured a positioning accuracy to within about 0.1 mm for the 2-mm-1/e-diameter beam.

Representative temperature-time histories of the endothelium that were measured using the thermocouple are shown in Fig. 3, wherein peak irradiance was 24 W/cm^2. The exposure durations in Figs. 3a and 3b were, respectively, nearly equal to and 10 times the epithelial damage threshold. The latter exposure was chosen because it is near the threshold for endothelial damage[6] (cf. Section 4.0). The curves in Fig. 3 are the values calculated from the model. The different temperature increases in Fig. 3a and in Fig. 2, both cor-
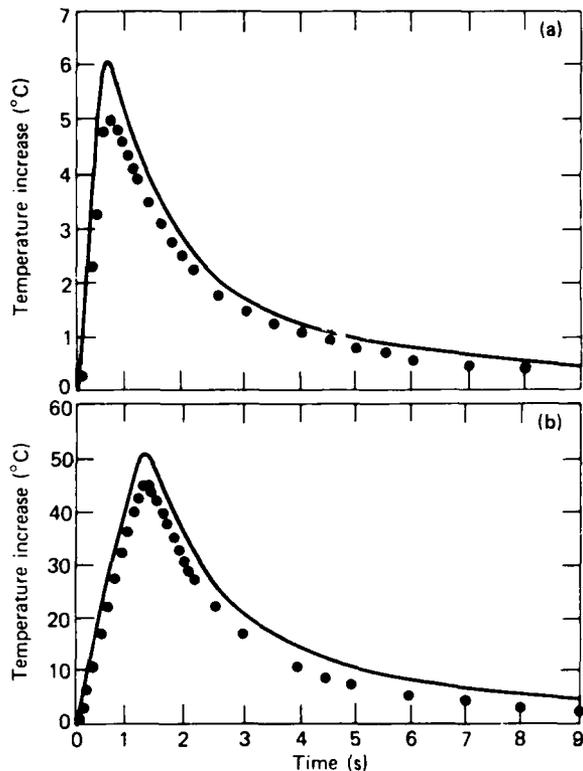
Figure 3 (a) The circles are measurements of the endothelial temperature increase as a function of time made with the 0.025-mm thermocouple positioned on the beam axis. The curve is the value calculated for the same position. The peak irradiance was 24.0 W/cm^2, the duration was 0.104 s, and the 1/e radius of the beam was 1.0 mm. The measured in situ corneal thickness was 0.38 mm. (b) The measured endothelial temperature increase as in (a) with the exception that the exposure duration was increased to 1.04 s. This exposure corresponds to the threshold for endothelial damage at this power density.[6]

responding to similar exposures, can be attributed to the different corneal thicknesses in the two experiments. If the thickness difference is taken into account, the two measuring techniques are in close agreement.

Figures 2 and 3 show that the measured temperatures are consistently somewhat lower than the temperatures calculated from the model. Nevertheless, the agreement is quite reasonable. Several factors associated with the temperature measurements (e.g., imperfect thermal contact between film or thermocouple and the cornea, finite response times, heat loss in the thermocouple leads, etc.), which were assumed to be small, all act to reduce the measured temperature. Also, as noted above in the

discussion of the theoretical model, the neglect of heat losses from the anterior surface via evaporation, convection, and radiation, as well as the latent heats associated with phase transitions, serves to make the calculations represent an upper bound to the actual endothelial temperature. Thus the good agreement achieved— even in the exposure of Fig. 3a, where all of these effects would have been most severe—justifies the approximations of the model.

Another approximation is the neglect of possible convective heat transfer at the endothelial surface. Indeed, we did observe convection in the sample cell while making the liquid crystal temperature measurements.[9] The Green's function solution assumes that the conduction equation holds across the endothelial boundary and that the cornea and bathing media have the same thermal properties. Convection currents would change the semi-infinite slab problem into a finite thickness slab problem with a convective boundary condition at the endothelial surface.[7-10] This boundary condition relates the temperature difference across the boundary to its normal derivative there. Conventionally, one assumes a linear proportionality (which introduces an unknown constant), and uses an eigenfunction expansion to calculate the temperature increases.[10] We did develop the expansion appropriate for both the uniform beam problem and the Gaussian beam problem,[9] and, as expected, the solutions showed a more rapid reduction in endothelial temperature after attainment of the peak value than for the more slowly cooling conducting case. However, no a priori procedure is available for determining the unknown proportionality constant. Although the constant could be "determined" a posteriori so as to give a best fit to the experimental data, we deem such an approach arbitrary, especially in view of the other approximations discussed above. Consequently, we elected to ignore possible convection currents and use the semi-infinite slab approximation for our calculations, particularly since this approximation is in such good agreement with the experiments.

[9]C. B. Bargeron, R. A. Farrell, W. R. Green, and R. L. McCally, "Structural Alterations in the Cornea from Exposure to Infrared Radiation," Annual Report to Letterman Army Institute of Research, Presidio of San Francisco, Calif. (Sep 1979).

[10]H. Y. Olcer, "On the Theory of Conductive Heat Transfer in Finite Regions with Boundary Conditions of the Second Kind," Int. J. Heat Mass Transfer **8**, 529-556 (1965).

4.0 ENDOTHELIAL DAMAGE THRESHOLDS

This research stemmed from a report that there was some evidence of altered endothelial integrity following laser exposures at, or slightly above, the threshold level for epithelial damage.[11] If correct, this observation could have clinical implications because, in primates and humans, endothelial damage is not believed to be repaired by cell division, but rather by the undamaged cells enlarging and sliding to cover the wound.[12] Thus the effect of repeated exposures could be cumulative and eventually the endothelium's ability to maintain normal corneal hydration (and therefore transparency) might be impaired.

Endothelial damage thresholds were determined for peak irradiances of 24.5, 10.0, and 3.6 W/cm.[6] The CO_2 laser was operated as usual in the TEM_{00} mode with a $1/e$ beam diameter of 2.0 mm. Exposure times were increased from values near the (then) known epithelial damage thresholds until we found the minimum time required to produce endothelial damage.

To detect endothelial damage, the rabbits were sacrificed with an intravenous injection of Nembutal® approximately 2 h postexposure. The globes were enucleated and the corneas were excised at the limbus. Damage was detected by wet staining the endothelium with alizarin red S and trypan blue dyes.[13] In some instances indocyanine green dye was used in place of trypan blue with equivalent results.[14] In this staining method alizarin red S dye clearly delineates the borders of both healthy and damaged cells, while trypan blue dye (or indocyanine green dye) penetrates those cells whose membranes have become leaky.

The damage thresholds for the three irradiance levels are shown in Fig. 4.[6] Results were obtained on several rabbits at each exposure level. The average thickness of the corneas was about 0.4 mm. The same exposure duration was found for threshold damage when the corneas were examined either 24 or 48 h after the 10-W/cm^2 exposure; thus, there are no apparent long-term effects beyond those evident at 2 h.
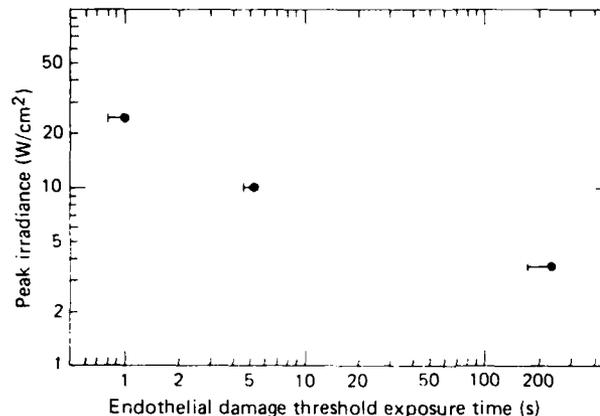
Figure 4 Peak irradiance versus endothelial damage threshold exposure time. The $1/e$ radius of the beam was 1.0 mm for all exposures. The circles indicate the minimum time for which we observed damage and the partial error bar extends to the longest exposure for which no damage was observed. Sixteen rabbits were used to determine the threshold at 3.6 and 10 W/cm^2; five rabbits were used at the 24.5-W/cm^2 condition.

Two hours after the cornea is exposed at the endothelial damage threshold, slit-lamp examination reveals severe corneal edema localized at the lesion and strong stromal light scattering to a depth of about ¼ to ⅜ the corneal thickness. The severity of the epithelial lesion and damage to the anterior stroma at these exposures depend strongly on the peak irradiance. At 24.5 W/cm^2 (1.04 s), the epithelium is destroyed and there is significant stromal cratering, whereas at 3.6 W/cm^2 (240 s), the epithelium is damaged, but not destroyed, and no stromal dimpling or cratering is evident. These observations are not surprising because calculations show that the thermal insult to the anterior cornea is much less severe for the 3.6-W/cm^2 (240-s) exposure than it is for the higher irradiance, but shorter duration, exposures.

The appearance of the endothelium for various exposure conditions is illustrated in Figs. 5, 6, and 7. Figure 5 shows the endothelium of a cornea 2 h after exposure to 10-W/cm^2 radiation for about 90% of the endothelial threshold damage time (i.e., for 4.56 s). The cells appear like those in control corneas and no damage is evident. This result also was found in corneas examined 24 and 48 h after similar exposures. The uneven focusing across the photograph is typical for these wet preparations, which are often not completely flat.

[11] E. S. Beatrice and B. E. Stuck, "Ocular Effects of Laser Radiation: Cornea and Anterior Chamber," *AGARD Lecture Series Vol. 79, Laser Hazards and Safety in the Military Environment,* p. 5 (1975).

[12] D. L. Van Horn and R. A. Hyndirck, "Endothelial Wound Repair in Primate Cornea," *Exp. Eye Res.* **21,** 113-124 (1975).

[13] D. J. Spence and G. A. Peyman, "A New Technique for the Vital Staining of the Corneal Endothelium," *Invest. Ophthalmol.* **15,** 1000-1002 (1976).

[14] J. K. McEnerney and G. A. Peyman, "Indocyanine Green—A New Vital Stain for Use Before Penetrating Keratoplasty," *Arch. Ophthalmol.* **96,** 1445-1447 (1978).

Figure 5 A photograph of endothelial cells near the beam axis. The peak irradiance was 10 W/cm², the duration was 14.56 s (corresponding to about 0.9, the damage threshold time), and the 1/e radius of the beam was 1.0 mm. The endothelial cells appear normal.

Figure 7 A higher magnification view of the region indicated by the arrow in Fig. 6.

Figure 6 A low magnification photograph of the endothelial surface of a cornea exposed to 10-W/cm² radiation for 5.24 s. The 1/e radius of the beam was 1.0 mm. This exposure was near the endothelial damage threshold. The outer circular ring defines a portion of the damaged *epithelial* surface as seen through the preparation. The inner circular region is the endothelial thermal lesion. The dark indocyanine green staining between points A and B is associated with a folding artifact and not with thermal damage. The arrow points to the region shown in Fig. 7.

Figure 6 is a low-magnification view of the cornea's posterior surface 2 h after irradiation at 10 W/cm² for 5.24 s, which is at (actually slightly above) the endothelial damage threshold. The extent of anterior corneal damage also can be seen through such preparations. At threshold exposures for endothelial damage, this view of the anterior damage usually shows two distinct concentric areas, the inner area probably being associated with the aforementioned stromal cratering. The endothelial lesion is represented by the circular region at the center of Fig. 6. The center of this lesion is not coincident with that of the anterior surface damage area (probably as a result of the preparation). Threshold endothelial damage is characterized by distorted cells and uneven staining of the cell borders. In particular, much of each damaged cell border is more heavily stained with alizarin red S than are normal cell borders; yet other parts of the damaged cell borders are often completely unstained. Figure 7 highlights these features. The location of the area depicted in Fig. 7 is indicated by the arrow in Fig. 6. Another common feature of these lesions is that the boundary between the damaged area and the region containing apparently normal cells is rather sharp (compare Figs. 6 and 7).

At exposures that are somewhat above threshold, endothelial cells at the center of the lesion are obliterated and cells immediately surrounding the bare region appear to have been pushed away from the center. Further outward, the cells look similar to those in a threshold lesion, and as with a threshold lesion, there is a sharp boundary with the undamaged area.

14

We found that alizarin red S stain gives the most useful damage information for thermal lesions of the endothelium. Trypan blue or indocyanine green staining is sporadic and sometimes absent.[5] When present, the staining is frequently associated with preparation artifacts such as folds (cf. Fig. 6).

The endothelial temperature increases on the beam axis were calculated for the threshold conditions of Fig. 4 and are shown as functions of time in Fig. 8. At threshold, the endothelium experiences peak temperature elevations of 30 to 50°C. These values are similar to those experienced by the epithelium at its damage threshold[3,4,11] (see also Section 7.0). Thus the endothelium's sensitivity to thermal insult is similar to that of the epithelium.

The data in Fig. 4 show that for a CO_2 laser with a 2-mm-$1/e$ beam diameter, the exposure durations required to cause threshold endothelial damage are about 10 times those required to produce threshold epithelial damage at the same irradiances. This result would not necessarily hold for other lasers or even for other exposure conditions with the CO_2 laser. Figure 9 illustrates this point for the CO_2 laser (wavelength, 10.6 μm), the holmium laser (wavelength, 2.06 μm), and the erbium laser (wavelength, 1.54 μm).[5,6] Differences in the results for the three lasers are caused by the marked variations in the corresponding absorption length of their radiation in the cornea (assumed to be the same as in water). (The absorption length is the inverse of the absorption coefficient in the exponential expression of the Beer-Lambert law. It is the distance into the medium at which 63.2% of the incident radiation has been absorbed.) The absorption lengths for holmium and erbium lasers are, respectively, 256 and 840 μm,[15] or about one-half and twice the corneal thickness; the value for the CO_2 laser is only 10.6 μm, or about one-fourth the thickness of the epithelium.[4]
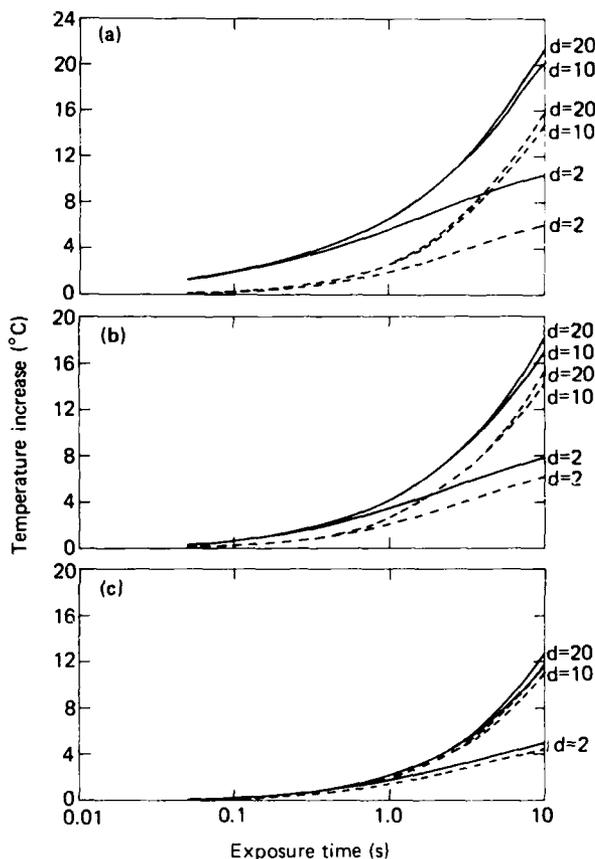
Figure 9 (a) Predicted temperature increase as a function of exposure time for a TEM_{00} mode CO_2 laser beam of peak irradiance 1 W/cm². Note that since the temperature increase is directly proportional to the peak irradiance, the increases for other values of peak irradiance can be found by multiplication. The solid curves represent temperature increases at a depth of 10 μm (anterior epithelium); the dotted curves, at a depth of 400 μm (endothelium for rabbit). The value of d, the $1/e$ diameter of the beam, is in millimeters. The absorption coefficient is 950 cm⁻¹ for 10.6-μm radiation. (b) Same as (a) except the conditions are for a holium laser (wavelength, 2.06 μm; absorption coefficient, 39 μm⁻¹). (c) Same as (a) except the conditions are for an erbium laser (wavelength, 1.54 μm; absorption coefficient, 11.9 μm⁻¹).

Figure 8 Calculated endothelial temperature histories for exposures of: a) 24.5 W/cm², 1.04 s; b) 10 W/cm², 5.24 s; and c) 3.6 W/cm², 240 s. At 240 s, curve c) reaches about 32°C as indicated by curve c′) and corresponding time scale along the top of the figure. A corneal thickness of 0.40 mm and a $1/e$ beam radius of 1.0 mm were was used in the computation. Zero time corresponds to the beginning of the exposure.

[15]K. F. Palmer and D. Williams, "Optical Properties of Water in the Near Infrared," *J. Opt. Soc. Am.* **64**, 1107-1110 (1974).

Figure 9 shows that the ratio of the exposure time needed to cause a given endothelial temperature increase to the exposure time needed to cause the same increase in epithelial temperature will decrease with increasing beam diameter and/or with increasing absorption length. For these curves the ratio is as small as 1.25 for the erbium laser and as large as 10 for a 2-mm-diameter CO_2 laser beam. The results in Fig. 9 also show that the ratio of the epithelial temperature increase to the endothelial temperature increase at a fixed exposure time decreases with increasing exposure time but is independent of the peak irradiance. Thus, for a given epithelial temperature increase, the concomitant endothelial temperature increase will be larger with a lower peak irradiance beam. Therefore, the characteristics of the infrared laser beam must be specified carefully when discussing potential hazards to endothelial cells.

5.0 STROMAL DAMAGE

During the investigation of endothelial damage we noted that corneas exposed at greater than the epithelial damage threshold, but less than the endothelial damage threshold, develop bowl-shaped lesions in the stroma that are nearly devoid of cells 48 h postexposure.[16,17] At that time, such corneas have recovered their normal thickness and have regrown a smooth epithelium. Figure 10, a montage of light micrographs, clearly shows this acellular region. The border between the damaged and undamaged region is sharply delineated. The abruptness of the demarcation suggested to us that keratocyte damage, like that of endothelial and epithelial cells, depends sensitively on the thermal insult.

To investigate this dependence, we exposed several corneas so that the damage extended about halfway through the stroma. Two exposure levels were investigated, one at 9.7 W/cm^2 (peak irradiance) for 2.5 s and the other at 26 W/cm^2 for 0.4 s. The $1/e$ beam diameters were 1.88 mm for the first exposure level and 2.44 mm for the second. The durations of both exposures are about four times longer than the duration required to produce minimal epithelial damage[3,4,17,18]

(see Section 7.0) and both exposures produced similar damage to the cornea. We took slit-lamp photographs within 1 h after the exposures and again at 48 h after which the rabbits were sacrificed and the exposed eyes were prepared for light and electron microscopy (see Ref. 17 for details). (A few animals were also sacrificed at 1 h.)

Figure 11 shows the appearance of the cornea at 1 and 48 h after an exposure to 26 W/cm^2 for 0.4 s. At 1 h, the slit lamp reveals a circular hazy lesion whose periphery is surrounded by a raised ring of epithelium. As noted above, by 48 h the cornea has regained its normal thickness, its front surface is covered by newly grown epithelial cells, and it is completely smooth. The circular hazy lesion remains. The bowl-shaped lesion is clearly visible in the narrow-slit photograph.

Figure 10, which was referred to above, is a composite light micrograph of a cornea exposed like the one in Fig. 11. The sections were cut as near as possible to a plane passing through the center of the circular damage area. The nearly cell-free lesion extends about halfway through the stroma at its deepest point. Transmission electron micrographs also were made of this lesion. Figure 12a shows that the basement membrane is intact. At this stage of healing, however, the basal epithelium is flattened and irregular. The anterior stroma shows a greatly reduced number of keratocytes. Those that remain appear necrotic with dark, dense, intracytoplasmic deposits, small vacoules, and a loss of normal intracytoplasmic organelles. The sharpness of the demarcation between damaged and undamaged stroma is clearly revealed at the higher magnification of Fig.

[16]R. L. McCally, C. B. Bargeron, W. R. Green, and R. A. Farrell, "Stromal Damage in Rabbit Corneas Exposed to CO_2 Laser Radiation," *Exp. Eye Res.* **37**, 543-550 (1983).
[17]R. A. Farrell, R. L. McCally, C. B. Bargeron, and W. R. Green, "Alterations in the Cornea from Exposure to Infrared Radiation," Annual Report to Letterman Army Institute of Research, Presidio of San Francisco, Calif. (Sep 1982).
[18]N. A. Peppers, A. Vassiliadis, L. G. Dedrick, H. Chang, R. R. Peabody, H. Rose, and H. C. Zweng, "Cornea Damage Thresholds for CO_2 Laser Radiation," *Appl. Opt.* **8**, 377-381 (1969).

Figure 10 A montage of light micrographs of a stromal lesion 48 h after an exposure of 26 W/cm^2 for 0.4 s. The 1/e radius of the laser beam was 1.2 mm. The nearly acellular lesion extends about halfway through the stroma and is bordered by normal (but perhaps slightly swollen) keratocytes.

(a) (b) (c)

(d) (e)
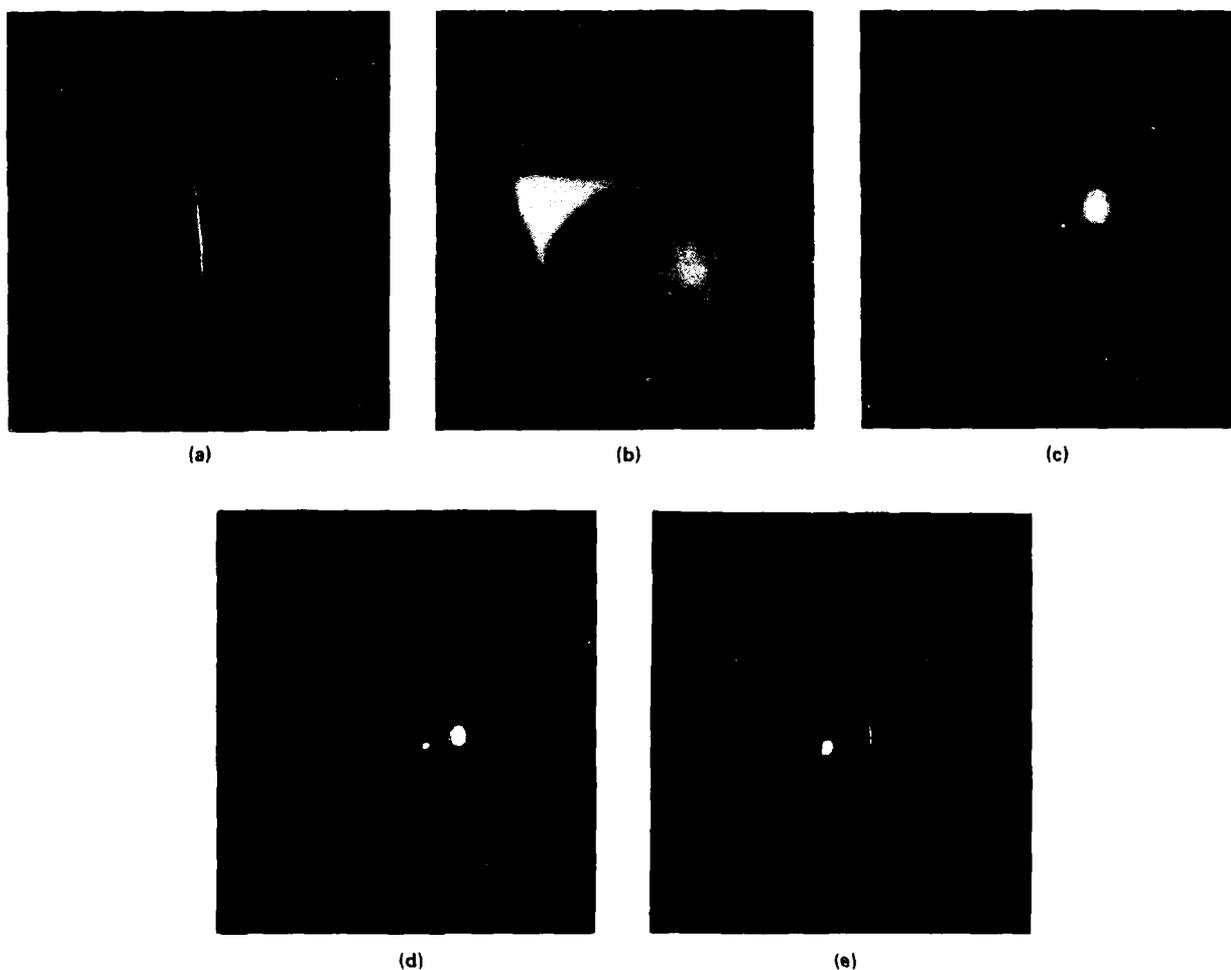
Figure 11 Slit-lamp photographs of a laser lesion caused by an exposure to a peak irradiance of 26 W/cm^2 for 0.4 s (1/e beam radius = 1.22 mm): (a) narrow slit, 1 h postexposure; (b) wide slit, 1 h postexposure; (c) wide slit, 1 h postexposure; (d) wide slit, 48 h postexposure; (e) narrow slit, 48 h postexposure.

Figure 12 (a) A low-magnification electron micrograph of the anterior stroma and epithelium of the cornea shown in Fig. 10. The basal epithelium is flattened and irregular, but the basement membrane is intact. The keratocytes that remain appear necrotic with dark, dense, intracytoplasmic deposits, small vacoules, and a loss of normal intracytoplasmic organelles. (b) A higher magnification electron micrograph of the same cornea showing the sharpness of the lesion edge. A necrotic keratocyte lies only 8 μm anterior to a completely normal keratocyte.

12b, which shows a necrotic keratocyte only 8 μm anterior to a completely normal keratocyte.

We used high-magnification slit-lamp photographs, taken just before sacrificing the animal for histology, to measure the shape of the lesion. The slit was made very narrow for these photographs and the lamp was arranged so that the light was incident normal to the cornea's surface. The narrow, illuminated region was positioned so that it passed directly through the center of the circular lesion, allowing us to obtain a cross section of the brightly scattering bowl-shaped lesion at its deepest point. The position of the lesion border was measured from the photographs and the depths were corrected for refraction at the anterior corneal surface. Figure 13 shows the border positions on two corneas with different exposures. The curves are calculated isotherms. For both exposures the lesion border closely follows the isotherms.

18
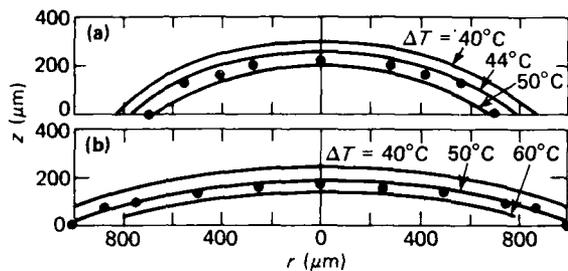
Figure 13 Measured position of the border of a bowl-shaped stromal lesion. The points are measured from a highly magnified slit-lamp photograph taken 48 h after an exposure of (a) 9.7 W/cm^2 for 2.5 s with a 1/e beam radius of 0.94 mm and (b) 26 W/cm^2 for 0.4 s with a 1/e beam radius of 1.21 mm. The curves are calculated isotherms.

Figure 14 Temperature histories at two positions on the isothermal surface having a 45°C temperature rise following a 9.7-W/cm^2-2.5-s exposure. The 1/e radius of the beam was taken as 0.94 mm. The solid curve is on the beam axis at a depth of 243 μm. The dashed curve is at a point 695 μm from the beam axis at a depth of 50 μm.

The calculations also reveal that the temperature history is similar at different positions on a given peak temperature isotherm. This is illustrated in Fig. 14, which shows the temperature histories for the 9.7-W/cm^2-2.5-s exposures at a point on the beam axis and a depth of 243 μm, and at a point having a radial position 695 μm from the beam axis and a depth of 50 μm. These two positions are both on the 45°C-peak-temperature isotherm. As expected, the temperature rise lags slightly for the deeper position, but the shape of the two curves is nearly identical. Similar results were obtained at other positions for this exposure and also for the 26-W/cm^2-0.4-s exposure.

These experiments show that the border of the stromal lesion produced by CO$_2$ laser irradiation is sharply delineated (as viewed in both the slit lamp and in the histologic sections) and that it corresponds to a surface of equal peak temperature rise. The conditions on this border represent the threshold for stromal cellular damage, which is at a slightly higher temperature for shorter exposure durations than it is for longer exposure durations.[16]

Similar peak temperatures and dependencies on exposure duration have been found for epithelial and endothelial damage[3,4,6,17,18] (also see Sections 4.0 and 7.0). Thus we conclude that all corneal cells have a similar thermal damage mechanism.

6.0 WOUND REPAIR

As discussed above, that corneas exposed above the threshold for epithelial damage, but below that for endothelial damage, develop a sharply defined bowl-shaped lesion, with borders corresponding to a surface of equal peak temperature increase within the stroma.[16,17] The peak temperature value depends on exposure duration, being slightly lower for longer exposures. Since similar peak temperatures and dependencies have been found for threshold epithelial and endothelial damage,[3,4,6,17,18] we concluded that all corneal cells have a similar thermal damage mechanism. Since the basement membrane did not seem to be damaged in these experiments,[16,17] at least up to 48 h postexposure (see Section 5.0), the time course of healing for this type of

19

wound was of considerable interest. Consequently, we extended our work on such exposures to document the healing process.[19,20]

All exposures were made on the central cornea using a $1/e$ beam diameter of 2.8 mm. The irradiance was fixed at 25 W/cm^2 and the exposure duration was 0.4 s. As noted in Section 5.0, this exposure level produces a wound that penetrates about halfway through the cornea at its deepest point. In the first series of experiments, 14 rabbits were exposed. Slit-lamp photographs were taken at 1, 24, and 48 h and at 1, 2, 4, and 8 weeks postexposure. Two rabbits were sacrificed at each interval and the exposed corneas were prepared for histological examination. Representative slit-lamp photographs and histological results are shown in Figs. 15 through 25. In a second set of experiments we exposed six more rabbits. Three of the rabbits were used for slit-lamp observation at 3, 4, and 5 days and one eye was prepared for histological examination at each of these times. The remaining three rabbits were used for slit-lamp observations up to 11 months postexposure.

Fig. 15a shows the appearance of the cornea at 1 h. The center of the wound is highly scattering, the central cornea is thickened and rough, and the epithelium is raised around the periphery of the lesion. There is a sharp transition from the damaged area to the clear, evidently undamaged, cornea. (Fig. 15a is similar to Fig. 11.) Figure 16 shows typical light micrographs of the wound area. In Fig. 16a, the damaged area extends about halfway through the stroma and also indicates the irregular roughening of the central ephithelium. The endothelium and Descemet's membrane appear normal. The transition from normal to burned epithelium is shown in Fig. 16c. The raised area, which is evident in the slit-lamp photograph, is clearly indicated. Inside this area the epithelium is thinned and darkly stained (see also Fig. 16b). In the electron microscope the epithelium shows marked disorganization, including nuclear chromatin clumping, loss of plasma membranes, and loss of cytoplasmic organelles (Fig. 19). The basement membrane looks undamaged. Figure 20 shows a necrotic keratocyte in the anterior stroma and abnormally fuzzy or smudged collagen fibrils.

The appearance of the cornea at 24 h is shown in Figs. 15b and 15c. In some cases at 24 h, the burned epithelium is completely opaque and has not yet peeled

off (cf. Fig. 15b), whereas in other cases, the burned epithelium has disappeared, revealing a brightly scattering wound in the stroma (cf. Fig. 15c, except that here, two small "flakes" of opaque material remain in the central area). Figure 17 shows that the wound is already covered by an immature epithelial layer that is only about 30 μm thick. The immature epithelium consists of basal cells, which have not yet attained their usual columnar form, covered by a single layer of superficial cells. These structures are seen in more detail in the electron micrograph of Fig. 21, which also shows some debris of keratocytes in the anterior stroma.

The acellular nature of the stromal wound at 48 h (discussed extensively in Refs. 16 and 17 in Section 5.0) is confirmed by the light micrograph shown in Fig. 17b. This micrograph also shows that the epithelium now has several layers of wing cells and that the columnar cells are better formed. The electron micrograph in Fig. 22 shows the new epithelium in more detail and reveals, as noted before, that the anterior stroma is devoid of cells. Only the debris of a few keratocytes remains.

The appearance of the lesion at 1 and 2 weeks is shown in Figs. 15d and 15e. At 1 week, the lesion looks very much as it does at 48 h. By 2 weeks, however, the anterior surface of the cornea is slightly flattened as a result of stromal thinning (cf. Fig. 15e) and the lesion is less visible in the wide-slit photograph of Fig. 15e. Histology reveals that the epithelium is completely normal at 1 week (Fig. 17c) and that the wound area is still acellular. The few dark staining areas are apparently debris of the necrotic keratocytes shown by the electron microscope (Fig. 23). By 2 weeks, however, the stroma is repopulated by keratocytes (Figs. 24 and 25) and the stromal collagen has regained its normal appearance (cf. Fig. 25).

The stromal thinning and anterior flattening are still evident at 4 and 8 weeks (cf. Fig. 15f and 15g). At 4 weeks there is still some scattering, but it is confined to the anterior-most portion of the stroma. The lesion remains faintly visible in the wide-slit photograph of Fig. 15f and is clearly visible in narrow-slit photographs. At 8 weeks the anterior scattering has diminished but is visible in the narrow-slit photograph of Fig. 15g. The hazy lesion is almost invisible in the wide-slit photograph of Fig. 15g. The light micrographs show that the keratocytes that have repopulated the lesion area continue to stain darker than normal (Fig. 18).

No involvement of vascular components (e.g., monocytes or polymorphonuclear leukocytes) or any vascularization was observed during the experiments. Also, the endothelium and Descemet's membrane remained normal throughout the 8-week period. The second series of experiments at days 3, 4, and 5 also failed to show

[19]R. A. Farrell, C. B. Bargeron, R. L. McCally, and W. R. Green, "Structural Alterations in the Cornea from Exposure to Infrared Radiation," Annual Report to Letterman Army Institute of Research, Presidio of San Francisco, Calif. (Jan 1985).

[20]R. L. McCally, C. B. Bargeron, W. R. Green, and R. A. Farrell, "Beam Diameter Dependence and Healing Processes in CO$_2$ Laser Damaged Corneas," Abs. Suppl., Invest. Ophthalmol. Visual Sci. 25, 328 (1984).

any evidence of inflammatory cells, which could have been missed in the first series of experiments. No remarkable evidence was uncovered as the second series

of rabbits was observed at 8 months and again at 11 months (the slit-lamp photographs of these rabbits up to 8 weeks were similar to those of the first set of rabbits). By 8 months, however, it was impossible to see the wound area using wide-slit illumination. In the narrow-slit view a very slight increase in scattering remained in the anterior-most region of the stroma. The stroma remained thin in this region, as had first been noted at 2 weeks. The general appearance of the corneas of these three rabbits was virtually the same at 11 months as it was at 8 months.
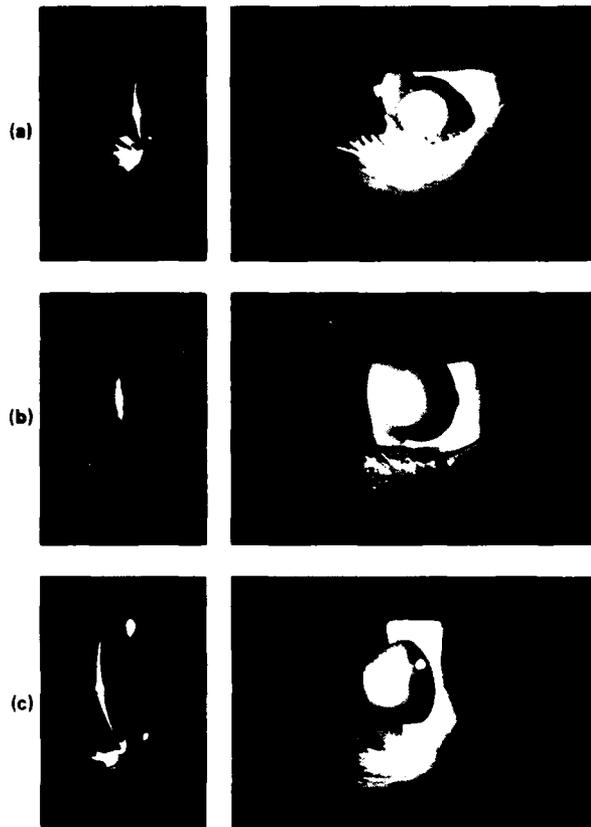
Figure 15 Slit-lamp photographs of laser-induced lesions produced by a 24-W/cm^2 peak irradiance and a 0.4-s duration. The 1/e radius of the beam was 1.4 mm, (a) At 1 h postexposure, a raised ring on the periphery of the lesion is typical. (b) At 24 h postexposure, the lesion is covered by the completely opaque, burned epithelium that has not yet sloughed off. About one-half of the rabbits have this appearance at 24 h. (c) Also at 24 h postexposure, the opaque covering has nearly sloughed off. There are two small "flakes" remaining in the center. (d) 1 week postexposure. (e) At 2 weeks postexposure, the stroma has thinned slightly in the center of the lesion, causing a flattening of the anterior corneal surface. (f) At 4 weeks postexposure, stromal thinning and anterior flattening are now quite evident. The stromal scattering is significantly reduced and is confined to the anterior-most region of the stroma. (g) At 8 weeks postexposure, the central area of the lesion remains thin and the hazy lesion is only faintly visible. Photographs (a), (e), (f) and (g) are all of the same rabbit.
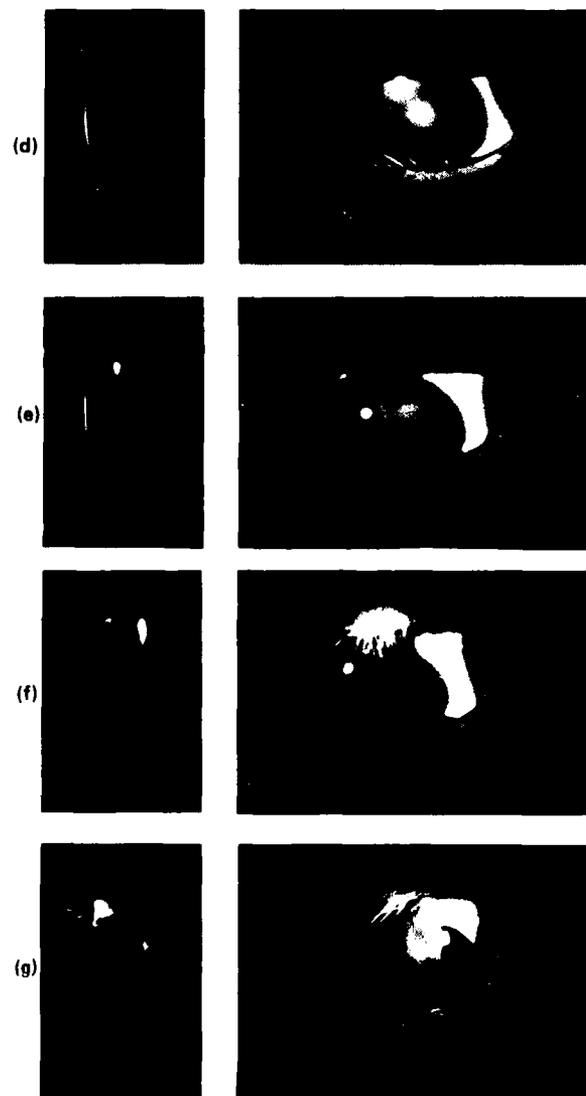
(a)
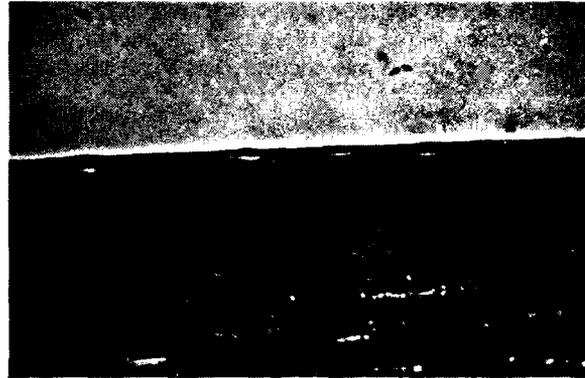
(b)
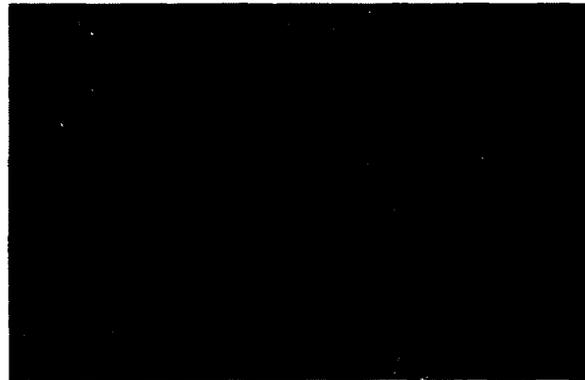
(c)

Figure 16 Light micrographs of laser-induced lesions after receiving exposures like those for the slit-lamp photographs (cf. Fig. 15). The 1-μm-thick Epon sections were stained with hematoxylin and eosin. At 1 hour, (a) the center of the lesion extends about halfway through the stroma. The central epithelium is highly disrupted and roughened. (b) The epithelium near the center is coagulated but smooth. (c) The edge of the lesion showing the transition between undamaged and damaged epithelium. The raised and disrupted edge that was evident in the slit lamp (cf. Fig. 15a) is shown clearly. The damaged epithelium stains very darkly and is significantly thinner, although all of the cell layers are evident.
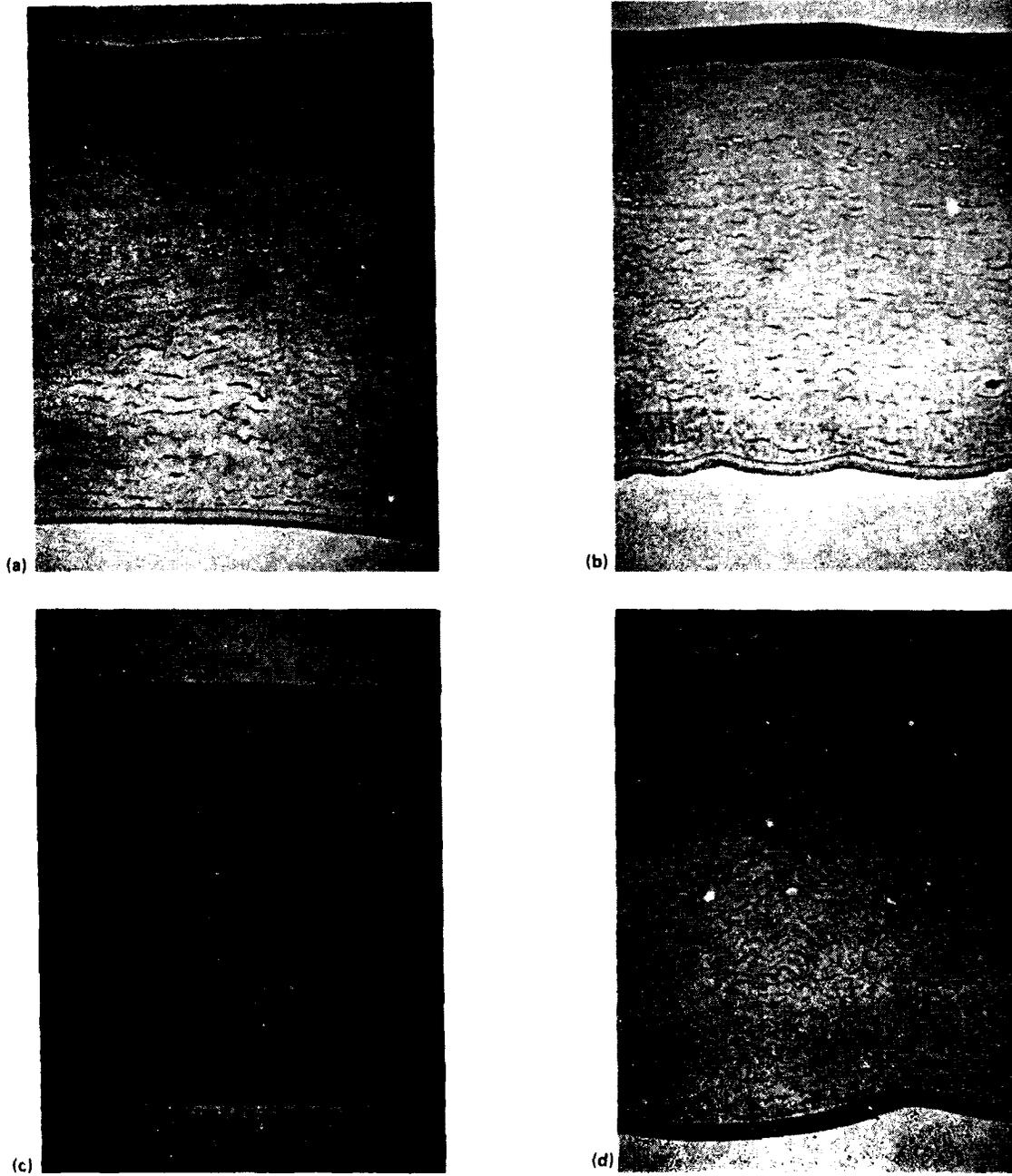
Figure 17 Same as Fig. 16. (a) The central area of the lesion at 24 h. The lesion is covered by a new epithelial layer; however, its basal cells have not attained their columnar shape and there is only a single layer of flat wing cells. (b) The central area of the lesion at 48 h. The basal cells are closer to their usual columnar form and there are several layers of wing cells. (c) The central area of the lesion at 1 week. The epithelium is normal in appearance. A few dark staining areas in the anterior stroma are evidently debris of damaged keratocytes. (d) The central area of the lesion at 2 weeks. The lesion is repopulated with keratocytes, which appear to stain more darkly than usual.

23

(a) **(b)**
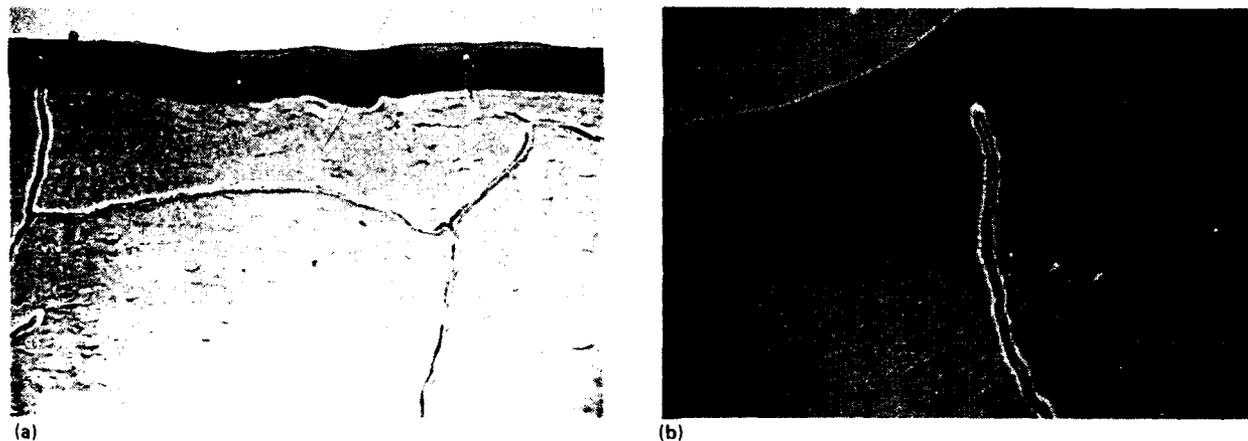
Figure 18 Same as Figs. 16 and 17. The central area of the lesion at (a) 4 and (b) 8 weeks. The kerato-cytes continue to stain darkly.

2 μm
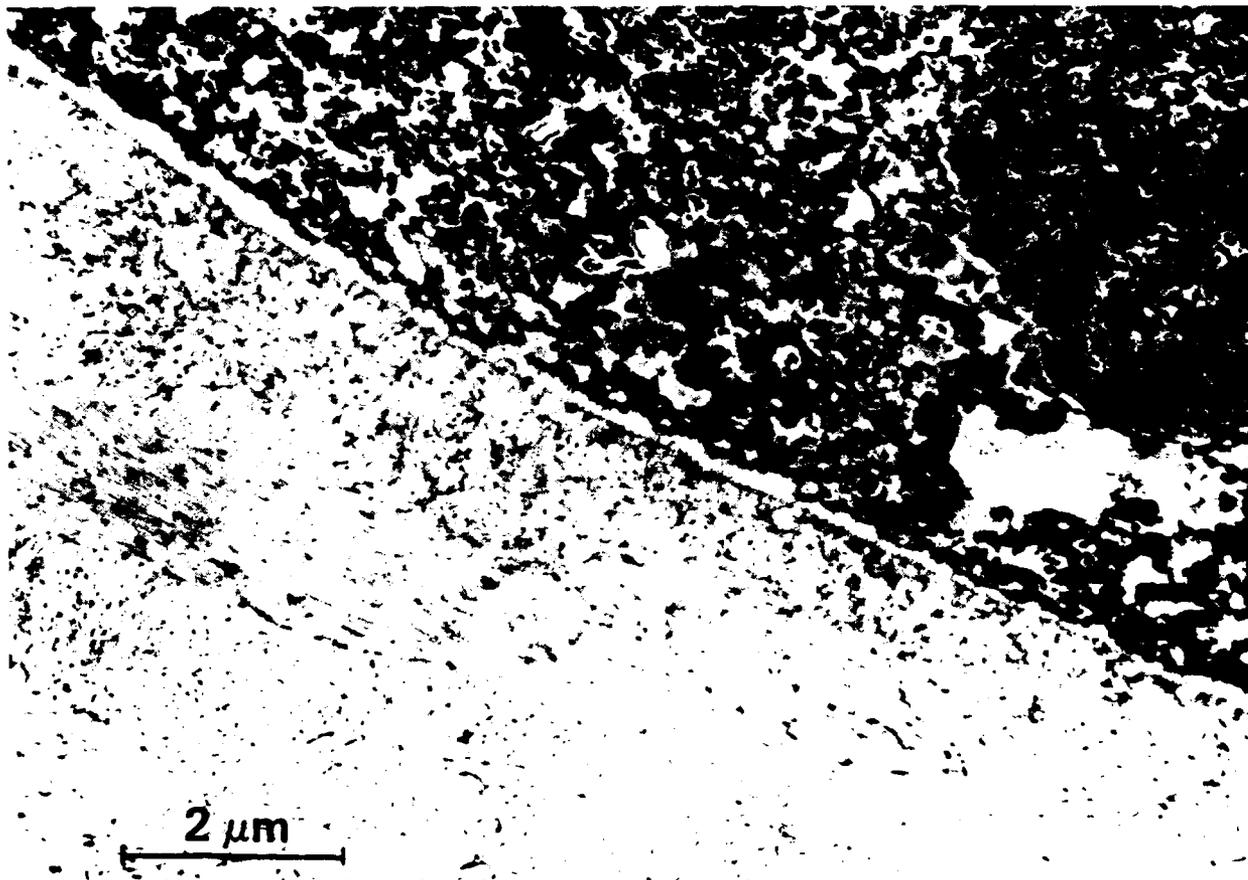
Figure 19 Electron micrograph of the epithelium and anterior stroma in the central lesion area at 1 h (cf. Figs. 15a and 16). The epithelium shows marked disorganization, including nuclear chromatin clumping, loss of plasma membranes, and loss of cytoplasmic organelles. The basement membrane appears to be undamaged.

24
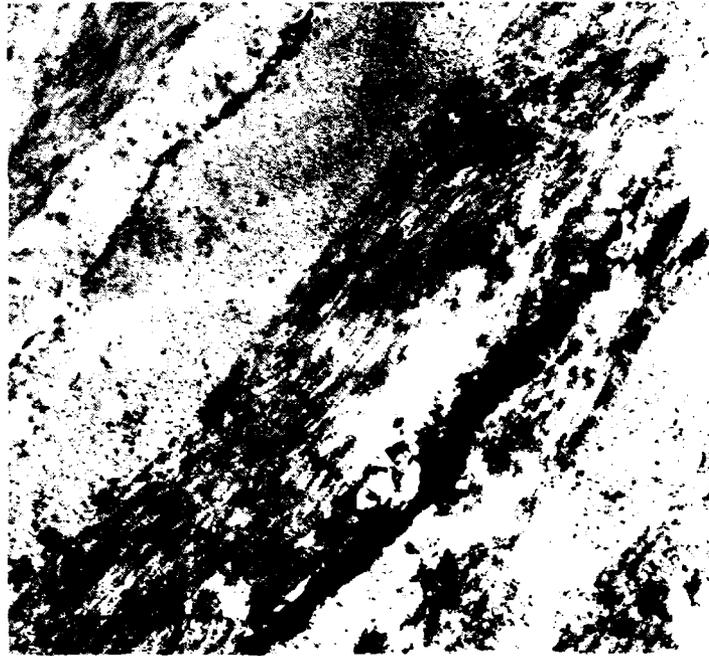
Figure 20   Electron micrograph of the anterior stroma in the central lesion area at 1 h showing a necrotic keratocyte (cf. Figs. 15a, 16, and 19). Note also the abnormal fuzzy or smudged appearance of the collagen fibrils.

Figure 21   Electron micrograph of the epithelium in the central lesion area at 24 h (cf. Figs. 15b, 15c, and 17a). The new epithelium consists of only two layers of cells. The basal cells have not attained their usual columnar form and there is only a single layer of flat wing cells. This micrograph also shows the debris of a few keratocytes in the anterior stroma.
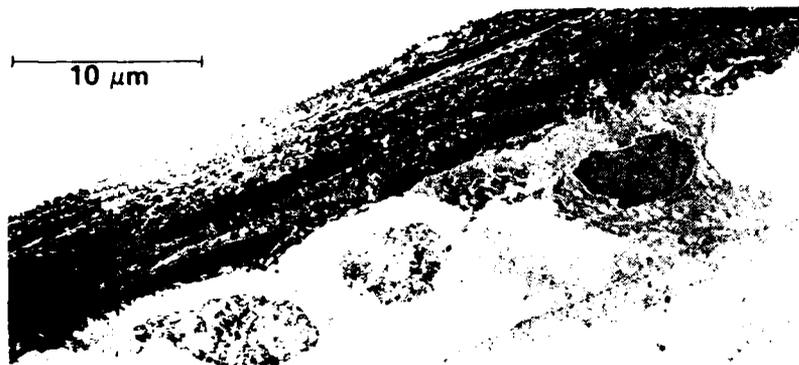
Figure 22 Electron micrograph of the epithelium and anterior stroma in the central lesion area at 48 h (cf. Figs. 10, 11e, and 17b). There are several layers of wing cells and the basal cells are better formed than at 24 h (cf. Fig. 21). The anterior stroma is devoid of cells; only the debris of necrotic keratocytes remains.
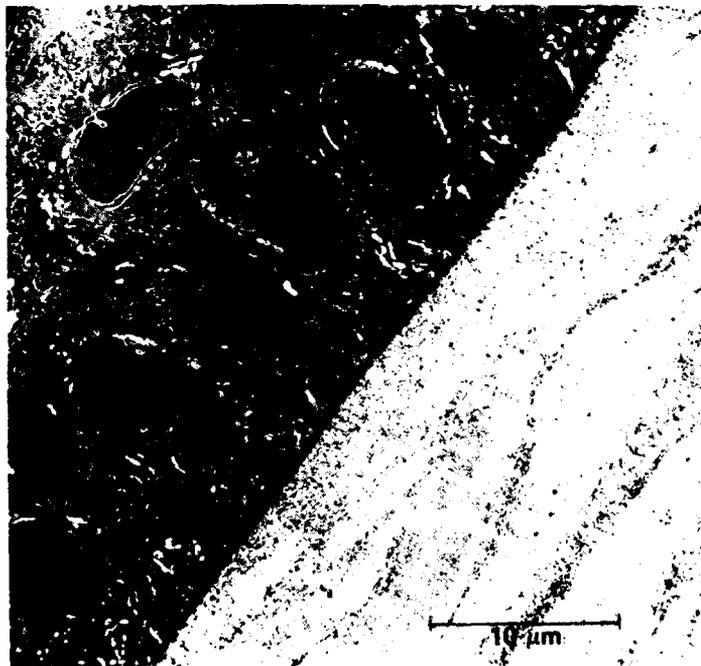
Figure 23 Electron micrograph of the epithelium and anterior stroma in the central lesion area at 1 week (cf. Figs. 15d and 17c). The basal cells are normal and the wound area remains acellular except for some debris.

26

Figure 24 Electron micrograph of the epithelium and anterior stroma in the central lesion area at 2 weeks (cf. Figs. 16e and 17d). The stroma is repopulated with keratocytes.
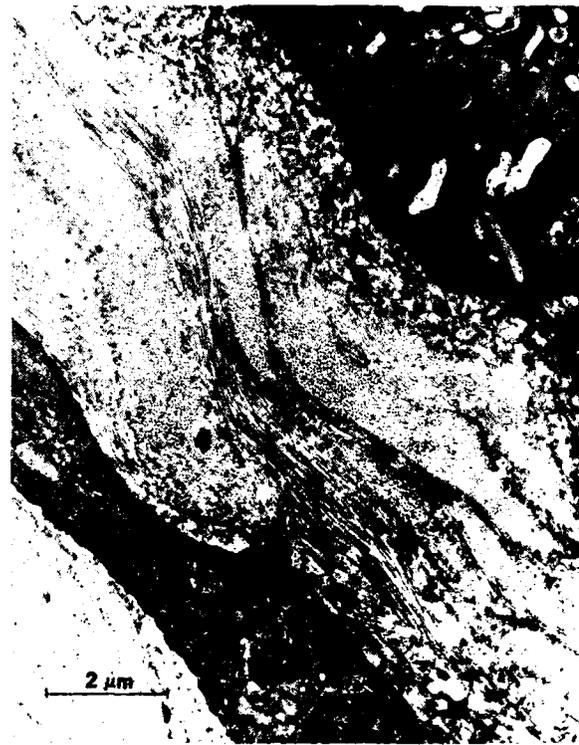
Figure 25 Electron micrograph of the basement membrane and anterior stroma in the central lesion area at 2 weeks (cf. Figs. 15e, 17d, and 24). The collagen fibrils have regained their normal appearance.

7.0 EPITHELIAL DAMAGE FROM SINGLE- AND MULTIPLE-PULSE EXPOSURES

This report has thus far dealt with thermal damage to the endothelium and stroma from CO_2 laser radiation; however, most of the work of others has concentrated on epithelial damage. This is natural, since 99% of the radiation from a CO_2 laser is absorbed within the first 50 μm of the tear film and epithelium. The energy is rapidly converted to heat that initially is concentrated in the volume of absorption. Many aspects of CO_2 laser damage to the corneal epithelium have been investigated over the past 15 years. Egbert and Maher[4] summarized the earlier work and discussed the empirical critical temperature and damage integral models for correlating threshold epithelial damage. The data they summarized came from many sources and covered a wide range of exposure parameters for single-pulse exposures (multiple-pulse data were not then availble in the literature). Although the data were somewhat scattered, Egbert and Maher found that both of these models could correlate the damage conditions.

An early formulation of the damage integral was made by Henriques,[21] who suggested that biological thermal damage depends on the integrated thermal history, weighted by an Arrhenius rate factor. He proposed the damage integral in the form

$$\Omega = A \int \exp(-B/T(t))dt , \qquad (1)$$

where A and B are constants and $T(t)$ is the absolute temperature of the tissue as a function of time. Threshold damage is reached when $\Omega = 1$. The constants A and B are to be determined from measurements of damage thresholds. The model was applied to corneal tissue by Brownell and Stuck.[3] It worked reasonably well for the earlier data; however, the values they found for A and B ($A = \exp(141.6)$ and $B = 48,400$ K) were such that their physical significance remained obscure.

The critical peak temperature (CPT) model was introduced by Egbert and Maher. In it, the threshold of damage was assumed to occur when the tissue was heated to a certain critical temperature. Egbert and Maher found it necessary to make the CPT a weak function of the exposure duration. Because the CPT is not constant it would perhaps be more accurate to say that they proposed a modified peak temperature model of damage. Nevertheless, they found that the equation

$$CPT = 79.6 \, \tau^{-0.0152} \qquad (2)$$

gave a good description of the existing data. In Eq. 2, the CPT is in degrees centigrade and τ is the exposure duration in seconds.

Both the damage integral and CPT models depend on being able to determine the temperature history at some position in the epithelium, which is usually accomplished computationally by solving the heat equation discussed in Section 3.0.

As noted above, previous studies have concentrated on damage caused by a single pulse of radiation from a CO_2 laser. In some applications, however, lasers are operated in a mode in which they emit a train of pulses. We have made the first measurements of epithelial damage thresholds for exposures to sequences of subthreshold pulses. We also obtained data for single-pulse exposures with durations ranging between 10^{-3} and 10 s using the same lasers, the same beam conditions, and

the same damage criterion to help us understand the multiple-pulse results. In addition, we measured the influence of beam diameter on single-pulse damage thresholds. By properly interpreting the measurements, we have provided corroboration of the modified critical temperature model for correlating damage. Moreover, certain aspects of the results with single-pulse exposures suggest a *new* physical model that can explain the slight variation in the CPT with exposure duration, at least for single-pulse exposures. The new model, which associates thermal damage with the occurrence of an endothermic phase transition, is discussed in Section 8.0.

We use the standard criterion for minimal epithelial damage, which is the presence of a superficial grayish white spot on the cornea that develops within 0.5 h of the exposure.[1,4] Corneas were assessed for damage by examination with a Nikon[*] photo slit lamp about 30 min after the exposure. For near-threshold damage, the faint spot is best located with a wide slit. Occasionally it was helpful to stain with fluorescein as a secondary method of damage assessment. After washing away residual stain, any thermal damage appears as a distinctive circular spot of diffuse fluorescence.

In practice, we find that the damage threshold is sharply defined, and we therefore do not use techniques such as probit analysis for its determination. Rather, we expose the tissue above threshold, then below. The gap above and below is narrowed to bracket the threshold condition. The final "bracket width" is such that the threshold value of irradiance is known to a precision of approximately $\pm 5\%$.

7.1 SINGLE-PULSE EXPOSURES

The experimental results for exposure durations, τ, between $\sim 10^{-3}$ and ~ 10 s are summarized in Table 1. The table also shows the peak temperature rise (above the ambient corneal temperature) on the beam axis 10 μm below the anterior corneal surface. The temperature was calculated using the Green's function solution discussed in Section 3.0. Although these temperature rises are nearly constant (especially in the range $10^{-2} \leq \tau \leq 1$, where they average $40 \pm 2°C$), the slight dependence on exposure duration noted by Egbert and Maher is obvious when the entire range is taken into account. The dependence of the peak temperature associated with damage on exposure duration is examined further in Fig. 26. In accordance with Egbert and Maher, we have plotted the natural log of the temperature (in degrees centigrade), and not the temperature increase. A value of $35°C$ is assumed for the ambient temperature of the cornea's anterior surface. A least

[21] F. C. Henriques, Jr., "Studies of Thermal Injury V. The Predictability and the Significance of Thermally Induced Rate Processes Leading to Irreversible Epidermal Injury," *AMA Arch. Pathol.* **43**, 489 (1947).

Table 1
Single-pulse exposures.

I_0 (W/cm^2)*	Pulse Duration (s)	ED_{th} (J/cm^2)	d (cm)	ΔT_{max} (°C)+
624	0.00096	0.599	0.102	54.0
177	0.0039	0.690	0.180	47.0
86.2	0.0092	0.790	0.252	41.4
64.3	0.0150	0.964	0.178	42.2
51.1	0.0185	0.945	0.180	38.1
57.2	0.0191	1.09	0.254	43.6
38.8	0.0309	1.20	0.260	39.5
20.4	0.101	2.07	0.158	39.5
8.99	0.498	4.48	0.182	37.9
9.39	0.500	4.69	0.224	41.0
6.46	0.977	6.31	0.244	38.3
2.89	9.730	28.1	0.248	34.1

*No errors are shown; however, the values are assumed to carry errors of ±10%. These reflect both the bracket spacing in determining the threshold (±5%) and the assumed accuracy of the power measurement (±5%). The same percentage errors would, of course, be reflected to ED_{th} and ΔT_{max}.

+ Maximum temperature rise calculated on the beam axis 10 μm beneath the cornea's anterior surface.

squares fit yields the (empirical) modified critical temperature model in the form

$$CPT = 72 \, \tau^{-0.02} \, °C \, , \qquad (3)$$

which is in close agreement with the correlation obtained by Egbert and Maher (cf. Eq. 2).

Theory predicts that the irradiance required to produce a given temperature rise for a given single-pulse exposure should depend on the diameter of the beam. Therefore, if a modified critical temperature model such as that in Eq. 3 were correct, epithelial damage thresholds should depend on beam diameter in the same way. We tested this prediction by measuring damage thresholds at a variety of beam diameters. Three exposure durations were used for the experiments: 0.1, 1.0, and 10 s. The experimental results are shown by the data points in Fig. 27, where the measured threshold irradiance is plotted as a function of beam diameter. Each of the three data sets shows that the irradiance required for threshold damage increases as the beam
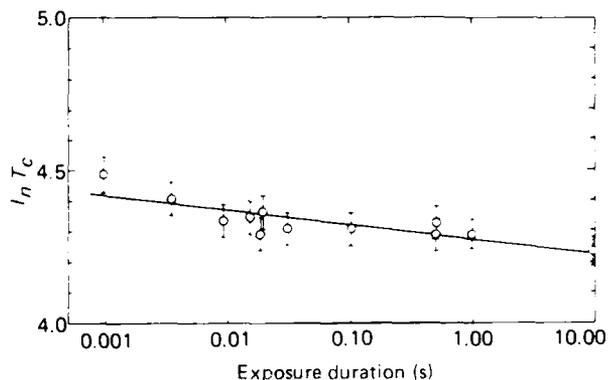
Figure 26 The natural log of the calculated temperature 10 μm beneath the cornea's anterior surface as a function of exposure duration. The ambient temperature of the cornea was assumed to be 35°C. The ±10% error bars reflect both the bracket spacing in determining the threshold and the estimated accuracy of the power measurement. The line is a least squares fit to the data and yields the empirical correlation given by Eq. 3.

29

diameter decreases. This result is attributable to radial heat conduction in the cornea, which becomes more important as the irradiated spot size decreases. If we were to assume that the modified *CPT* model were correct, then we could calculate the peak irradiance needed to cause this temperature rise as a function of beam diameter. The curves in Fig. 27 are the results of such calculations. For the 0.1-s exposures, the curve is for the peak irradiances needed to cause a 41°C peak temperature rise at a depth of 10 μm along the beam axis. The curves through the 1.0- and 10-s exposure data are for the irradiances needed to produce peak temperature increases of 39° and 36°C, respectively. In all cases the peak temperature increases are close to the values in Table 1 for the respective exposure durations and are therefore in close agreement with the correlation given in Eq. 3.

The relationship in Eq. 3 is, of course, only an empirical correlation of the damage data. To gain physical insight into the basis for the slight dependence of the *CPT* on exposure duration, it is helpful to examine how the energy density needed to cause minimal damage, ED_{th}, depends on exposure duration. The values of ED_{th} from Table 1 are displayed graphically in Fig. 28 as a function of exposure duration. The values of ED_{th} and their associated exposure durations are experimental data (peak energy densities of the Gaussian profiles) and are therefore independent of any thermal model assumed for temperature calculations. Our interpretation of this plot, however, assumes either that all the data are for the same diameter laser beam or that the data are obtained under conditions for which the irradiance required to produce damage is independent of beam diameter (cf. Fig. 27). At very short exposures, ED_{th} appears to be asymptotically approaching a fixed value. This behavior might be expected if the occurrence of an endothermic phase transition within the epithelium were the underlying damage mechanism. In that case, a *thermally isolated* epithelium would sustain damage when it absorbed enough energy both to raise its temperature to the transition temperature and then to supply the latent heat needed to cause the phase change (e.g., protein denaturation, alterations of the organization of the lipids in the cell membranes, etc.). For a thermally isolated epithelium, ED_{th} would be constant and independent of the exposure duration. Very short exposure durations approximate thermal isolation since the heat does not have sufficient time to be conducted away. Indeed, for the cornea, a characteristic conduction time associated with CO_2 laser radiation has been given as approximately 10^{-4} s.[22] This time is consistent with the

[22]M. L. Wolbarsht, "Laser Surgery: CO_2 or HF," *IEEE J. Quantum Electron.* **QE-20**, 1427-1432 (1984).
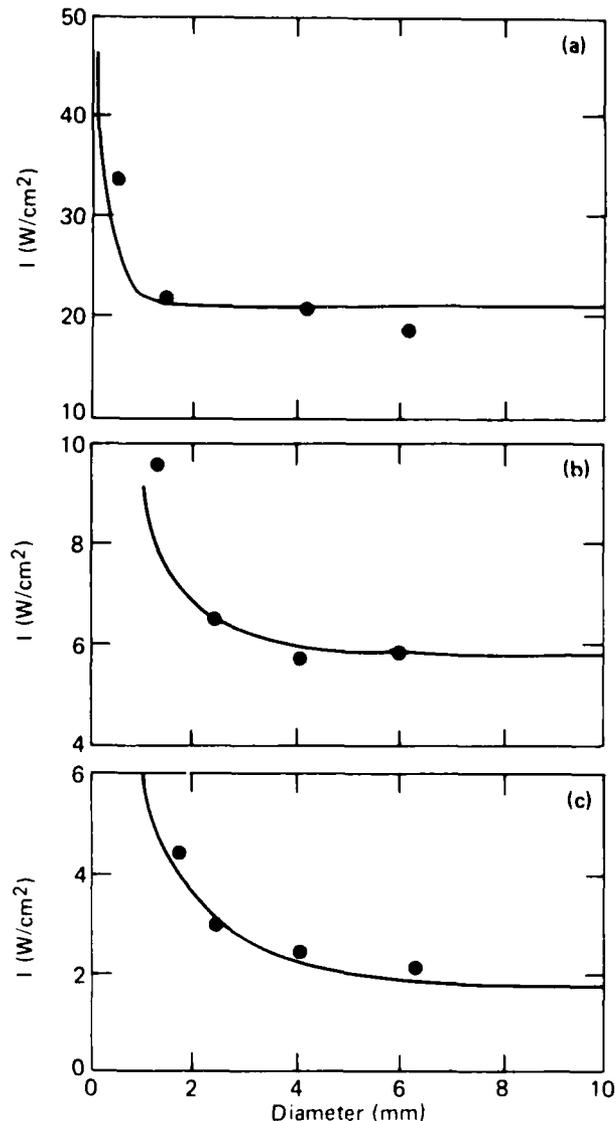
Figure 27 The data points are the experimental peak irradiances required to produce threshold damage as a function of beam diameter. The exposure durations were (a) 0.1 s, (b) 1.0 s, and (c) 10.0 s. The curves are the calculated peak irradiances needed to produce a fixed temperature rise, ΔT_c, at a point on the beam axis 10 μm deep into the epithelium. $\Delta T_c = 41°C$ in (a), 39°C in (b), and 36°C in (c).

apparent asymptotic limit suggested in Fig. 28. For the exposure durations in the present experiments, some of the energy would flow out because of conduction into the stroma. Thus more energy would have to be supplied to compensate for energy lost through conduction.
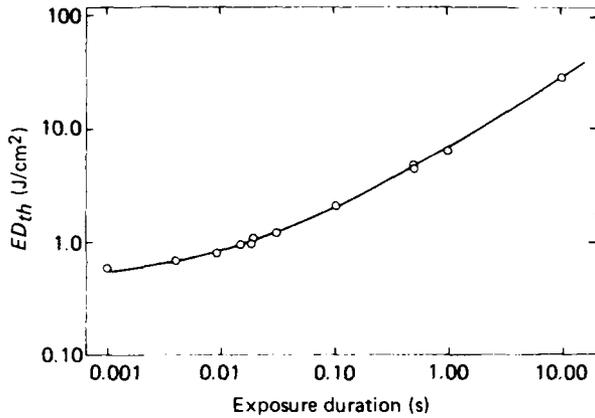
Figure 28 Energy density at the epithelial damage threshold, ED_{th}, for single-pulse exposures as a function of exposure duration. ED_{th} appears to asymptotically approach a fixed value at very short exposures.

We have incorporated these ideas into a *new physical* model to explain thermal damage. Because of its importance, we have chosen to discuss it separately in Section 8.0.

7.2 MULTIPLE-PULSE EXPOSURES

The specification of exposure conditions for multiple-pulse exposures is considerably more complex than for single pulses. In addition to the peak irradiance along the beam axis, I_0, the $1/e$ diameter of the beam, d, and the duration of the individual pulses, τ (all of which were required to specify the single-pulse experiments), the total number of pulses, N, and the pulse repetition frequency, PRF, must also be specified.

In the first series of experiments that we performed (Series 1), we held I_0, d, N, and PRF fixed, while τ was varied to determine the damage threshold. The procedure was repeated as I_0, N, and PRF were varied systematically. The results of these experiments are listed in Table 2, where it is apparent that threshold damage occurs when the maximum temperature increase is approximately 45°C. The temperature-time histories that correspond to the experimental parameters show a wide variability, as indicated in Fig. 29. The illustrated temperatures are those on the beam axis 10 μm below the anterior surface and have been calculated using an extension of the time-dependent Green's function solution discussed in Section 3.0.[23] Curves are presented for pulse trains containing between one and eight subthreshold pulses having peak irradiances of ~10 W/cm^2. The time histories for these exposures are sufficiently varied that they can be used to rule out the damage integral model (at least in the form of Eq. 1). Although that model could be used to correlate damage from single pulses, it does not apply for multiple-pulse exposures because no single set of values of the parameters A and B can be found for these exposure conditions.

Most of our experiments with multiple pulses, however, have concentrated on a different experimental protocol (Series 2). In Series 2 we held d, τ, and PRF fixed. As the number of pulses in the sequence was varied, we determined the minimum value of peak irradiance required to produce damage. Thresholds were determined in this manner for several values of PRF and for two values of τ. The results are compiled in Table 3, together with the computed value of the peak temperature increase on the beam axis 10 μm beneath the anterior surface.

Table 2
Multiple-pulse exposures (Series 1).

PRF (Hz)	Number of Pulses	I_0 (W/cm^2)	Individual Pulse Duration (s)	ED_{th} (J/cm^2)	Plot Symbol in Figs. 31 and 32	d (cm)	ΔT_{max} (°C) *
1	1	9.39	0.500	4.69	×	.224	41.0
1	2	9.82	0.370	7.26	×	.222	44.6
1	4	9.73	0.270	10.5	×	.220	42.2
1	8	11.2	0.240	21.4	×	.206	48.3
10	8	10.6	0.080	6.78	×	.210	47.3

*Maximum temperature rise calculated on the beam axis 10 μm beneath the cornea's anterior surface (cf. Fig. 8).

[23]P. M. Morse and H. Feshbach, *Methods of Theoretical Physics*, McGraw-Hill, New York (1953).
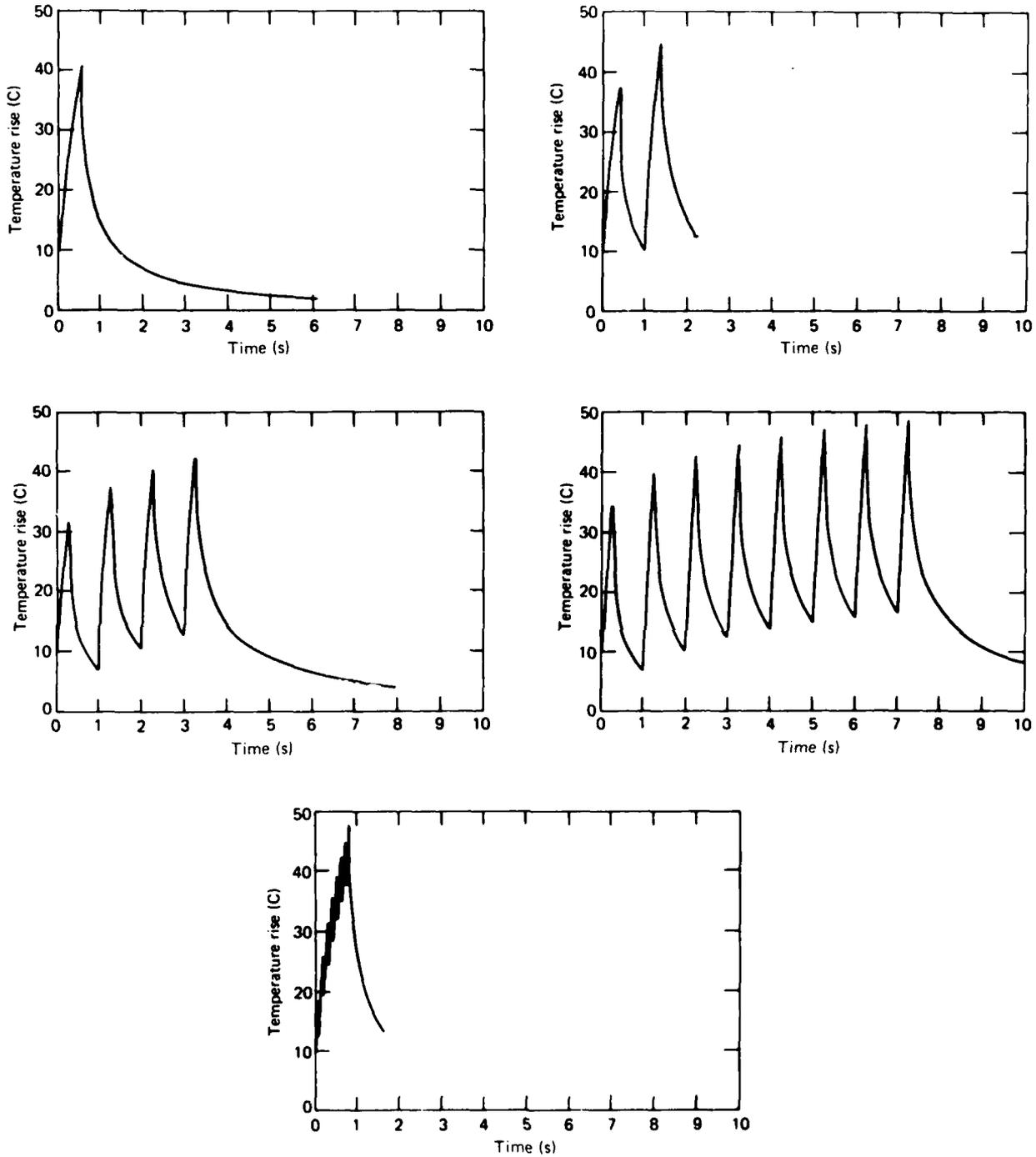
Figure 29 Calculated temperature-time histories at a depth of 10 μm along the beam axis for the multiple-pulse damage thresholds listed in Table 2.

Table 3
Multiple-pulse exposures (Series 2).

PRF (Hz)	Number of Pulses	I_0 (W/cm^2)	Individual Pulse Duration (s)	ED_{th} (J/cm^2)	Plot Symbol in Figs. 30, 31, and 32	d (cm)	ΔT_{max} (°C)
1*	1	86.2	9.2×10^{-3}	0.79	○	0.252	41.4
1	4	79.6	10.1×10^{-3}	3.21	○	0.172	43.4
1	32	66.8	9.3×10^{-3}	19.9	○	0.250	38.4
10	4	60.0	9.7×10^{-3}	2.32	□	0.256	43.3
10	32	32.7	10.9×10^{-3}	11.4	□	0.244	44.7
10	128	25.3	9.2×10^{-3}	29.8	□	0.270	39.8
20	4	55.3	10.0×10^{-3}	2.21	◇	0.252	46.4
20	32	27.8	9.9×10^{-3}	8.82	◇	0.240	47.7
20	128	16.4	8.9×10^{-3}	18.7	◇	0.276	38.8
1*	1	624	0.96×10^{-3}	0.599	△	0.102	54.0
20	10	239	0.94×10^{-3}	2.24	△	0.186	34.7
20	100	171	0.95×10^{-3}	16.3	△	0.174	39.0
20	500	122	0.92×10^{-3}	56.0	△	0.190	33.0
100	10	153	0.96×10^{-3}	1.47	▲	0.202	36.0
100	100	59.6	0.95×10^{-3}	5.67	▲	0.196	35.2
100	999	42.0	0.96×10^{-3}	40.3	▲	0.174	40.1

* From Table 1.
+ Maximum temperature rise calculated on the beam axis 10 μm beneath the cornea's anterior surface.

Because of the complexity of the temperature-time histories for experiments with multiple pulses, it is not as straightforward a problem to deduce a general damage correlation as was done for experiments with single-pulse exposures. In those experiments, the temperature increases monotonically with time until (depending on the particular thermal model) damage occurs or the critical temperature of the phase transition is reached (see Section 8.0). With multiple-pulse exposures, the temperature cycles up and down with the pulses, reaching a somewhat higher value after each successive pulse. Still, it is apparent that the maximum temperature increases reached at the end of the pulse sequence are all at least close to the values associated with damage in the single-pulse experiments. As noted above, this observation, and the extreme variability of the temperature-time histories, rules out the possibility that the damage could be correlated by the damage integral model (recall Eq. 1) since it is impossible to find a single set of parameters to satisfy the condition.

Damage from multiple-pulse exposures to the retina has been examined at Letterman Army Institute of Re-

search,[24,25] where it was found that $ED_{th} \propto N^{-}$. This empirical relationship is examined in Fig. 30 for the data in Table 3. The values of ED_{th} are plotted as a function of the number of pulses on a logarithmic plot. A line having slope ¾ is shown for comparison. Although there is wide scatter, the data can be correlated, at least roughly, in this manner.

Since the contract period covered by this report, we have reanalyzed the data in order to determine whether the damage is correlated by an approximate critical temperature law or by some form of the modified critical temperature law. In Fig. 31 we have plotted $\ln T_{max}$ (where $T_{max} = \Delta T_{max} + 35°C$) as a function of the total duration of the pulse train for each of the multiple-

[24] B. E. Stuck, D. J. Lund, and E. S. Beatrice, *Repetitive Pulse Laser Data and Permissible Exposure Limits*, Institute Report No. 58, Letterman Army Institute of Research, Presidio of San Francisco, Calif. (Apr 1978).

[25] D. J. Lund, B. F. Stuck, and E. S. Beatrice, *Biological Research in Support of Project MILES*, Institute Report No. 96, Letterman Army Institute of Research, Presidio of San Francisco, Calif. (Jul 1981).

33
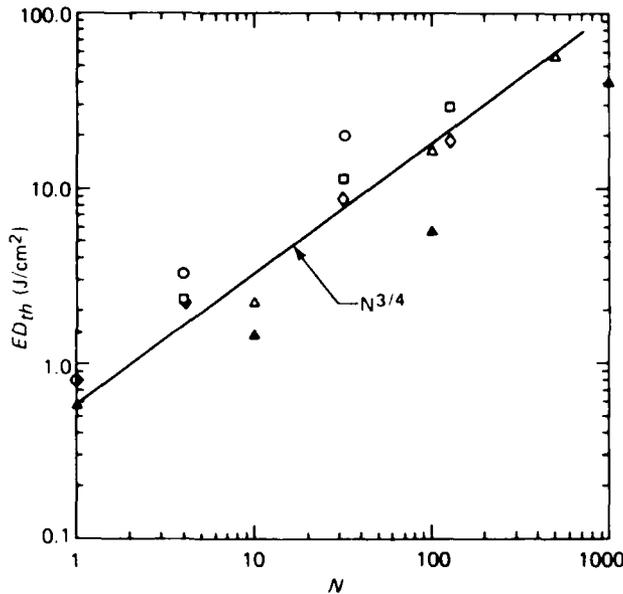
Figure 30 Energy density at threshold, ED_{th}, as a function of the number of pulses, N, for the data in Table 3. The line has slope ¾, suggesting that the multiple-pulse data are approximately correlated by a relationship $ED_{th} \propto N^{¾}$. A similar correlation has been suggested for a multiple-pulse damage to the retina.[24-25]
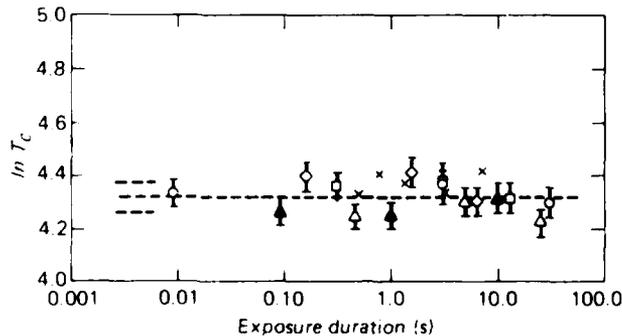
Figure 31 This plot is similar to Fig. 26 except that the data are for the multiple-pulse exposures in Tables 2 and 3. Here the log of the temperature on the beam axis 10 µm beneath the cornea's anterior surface is plotted as a function of the total duration of the pulse train. The ± 10% error bars reflect both the bracket spacing in determining the threshold and the estimated accuracy of the power measurement. Unlike the single-pulse data in Fig 26, there is no evident trend with exposure duration. The data scatter about the mean critical temperature, T_{max} = 75° (corresponding to a mean temperature increase of 40 ± 4°C).
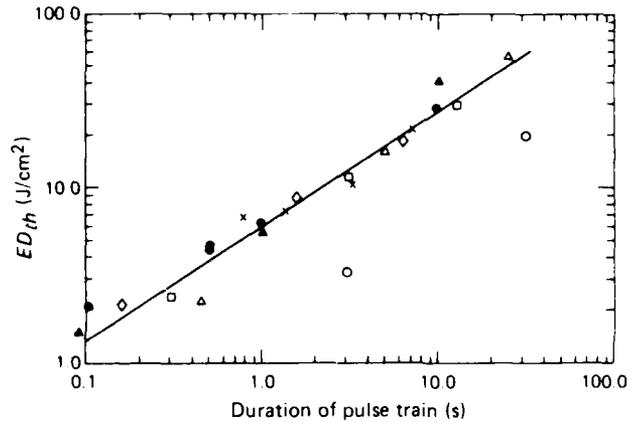
Figure 32 Energy density at threshold, ED_{th}, for the multiple-pulse exposures in Tables 2 and 3 as a function of the total duration of the pulse train. For durations longer than 0.1 s, the data are correlated by an empirical power law of the form $ED_{th} \sim D^{0.66}$. The plot symbols correspond to the respective conditions defined in Tables 2 and 3. The solid circles are for the single-pulse exposures that have durations of greater than 0.1 s (cf. Table 1).

pulse experiments in Tables 2 and 3. The total duration of the pulse train is given by $D = (N-1)/PRF + \tau$. While there is some scatter of the values of $\ln T_{max}$ about the mean, there is no trend of the data with D. This suggests that, to first order at least, multiple-pulse damage thresholds can be correlated by a critical temperature law in which damage is associated with a mean temperature increase of 40 ± 4°C (T_{max} = 75 ± 4°C). The correlation excludes the result for the *single* 1-ms pulse.

A different, but still empirical, correlation of the multiple-pulse data is given in Fig. 32. This method, also developed after the contract period covered by the present report, is included here for completeness. For durations, D, greater than ~0.1 s, the energy density at threshold, ED_{th}, is seen to obey a power law of the form

$$ED_{th} = (\text{const}) \, D^{0.66} . \tag{4}$$

This correlation depends only on measured, not calculated, parameters. It is not apparent why the points represented by open circles (corresponding to the experiments for which PRF = 1 Hz, $\tau \approx$ 10 ms, and N = 1, 4, and 32) do not lie on the same curve as all the

other data. However, the two points for which $D >$ 0.1 s lie parallel to the straight line formed by the rest of the data, indicating that the power-law dependence is the same. We also have included ED_{th} for the single-

pulse exposures having durations of ≥ 0.1 s on the plot (solid circles). (These points are the same as in Fig. 28.) It is evident that they cluster with the multiple-pulse data and appear to be asymptotic to the $D^{0.66}$ line.

8.0 THERMAL DAMAGE MODEL

In the section above, we noted that certain aspects of the epithelial damage data for single-pulse exposures are consistent with the hypothesis that damage is associated with an endothermic phase transition (see the discussion pertaining to Fig. 28 in subsection 7.1). We have incorporated this idea into a new thermal model that provides a physical basis for correlating epithelial damage data from single pulses. This model explains the slight variation in the CPT that was noted by Egbert and Maher[4] in terms of heat conduction into the cornea during the phase transition.

We consider the one-dimensional thermal model shown in Fig. 33, in which a uniform flux of radiation, F_0, is incident on a layered cornea whose initial temperature is T_0. The model is simplified further by assuming that the incident flux is absorbed in an infinitesimally thin section at the anterior surface of the epithelium (the tear film is neglected in this simple model). If the thermal properties of the various corneal layers were identical, then this problem would be that of the classical semi-infinite slab whose surface temperature increases as the square root of time as illustrated in Fig. 34a. The amount of heat conducted into the inner layers of the cornea depends on the derivative of temperature with respect to depth, which, for the simple slab, adjusts itself so that all of the incident flux is transported into the cornea.

Our new model differs from the simple slab by postulating that an endothermic phase transition occurs once the anterior surface reaches the transition temperature denoted by T_t in Fig. 34b. The time at which the front surface first reaches the temperature, T_t, is denoted by t_t. Just as a water-ice mixture stays at $0°C$ during melting, the surface temperature stays at T_t while the postulated endothermic transition occurs (see Fig. 34b). As a working hypothesis, we assume that observable damage is associated with a specific amount
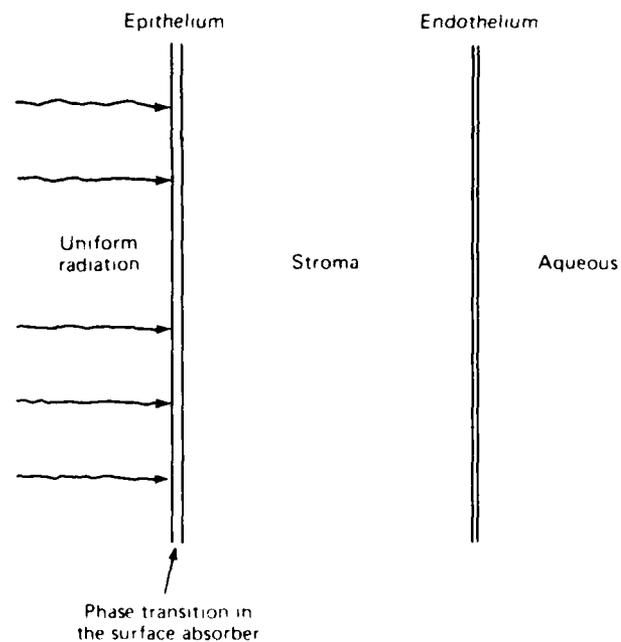
Figure 33 The geometry of a thermal model in which a uniform heat flux is incident on a surface absorber that can undergo an endothermic phase transition.

of material per unit surface area undergoing the transition, i.e., after a specific quantity of heat per unit surface area, Q_t, is absorbed in the phase transition.

For an exposure duration, τ (greater than t_t), the amount of heat per unit surface area, q, that actually goes into the transition is obtained by integrating the difference between the incoming flux, F_0, and the quantity of heat per unit area that is conducted into the cornea ($K \, \partial T / \partial x |_0$) from time, $t = t_t$, to τ. Here K is the thermal conductivity and the derivative

is evaluated at the front surface. For this particular model, the integral can be done analytically, yielding
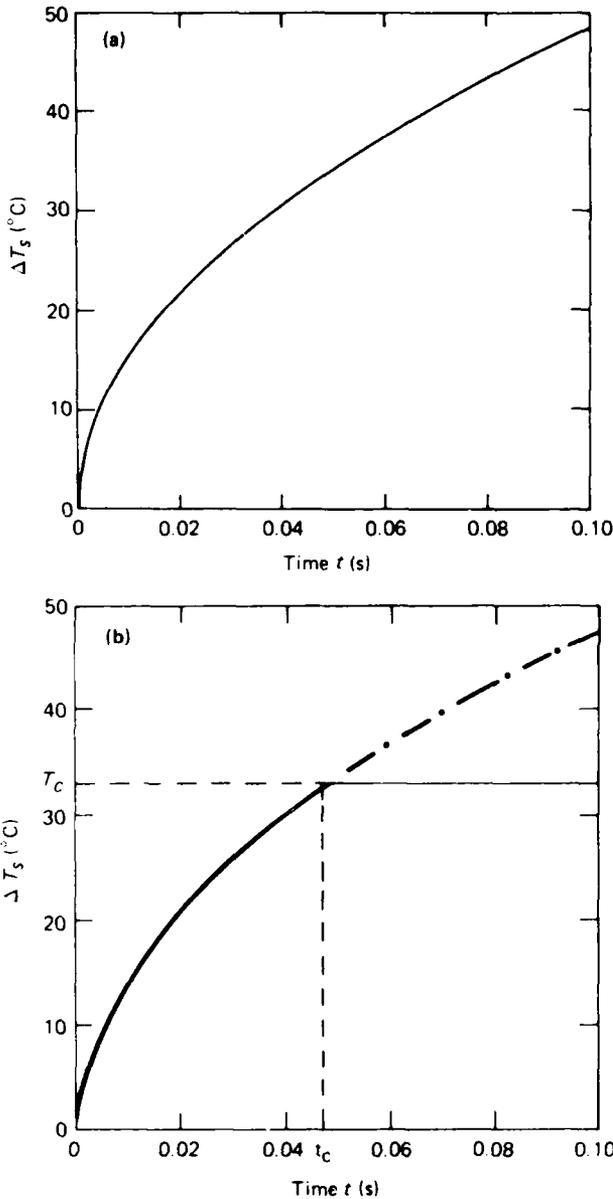
Figure 34 The increase in surface temperature as a function of time for the one-dimensional model of a surface absorber. (a) No phase transition takes place and the temperature increases as $t^{1/2}$. (b) The same as (a) except that an endothermic phase transition with a critical temperature of 33°C above ambient occurs. The surface temperature would rise as $t^{1/2}$ until t_c and then stay constant until the latent heat is supplied.

$$q = \{[1 + \theta^2](\tan^{-1}\theta) - \theta\}$$
$$\times \{[K(T_c - T_0)]^2\}/[2F_0\kappa] , \qquad (5)$$

where $\theta = [(\tau - t_c)/t_c]^{1/2}$, and κ is the thermal diffusivity (i.e., $\kappa = K/\rho c$, where ρ is the density and c is the heat capacity).

This model differs from the one-dimensional models that have been developed to examine laser damage in solid state devices.[26,27] Those models, like ours, account for heat conduction while the temperature of the material is increasing. However, they account for the endothermic phase transition by adding the energy necessary to vaporize the material instantaneously; thus, they ignore heat conduction occurring during the phase transformation. In applying our new model, as discussed below, we find that for exposures in the 1-ms range, the time required for the phase transition to occur can be as much as 60% of the total exposure duration. Thus the simplification that would be afforded by assuming an instantaneous phase transition is not justified in the analysis of our experiments.

If the transition temperature, T_c, and heat of transition, Q_c, were known, then Eq. 5 could be used to predict the thermal flux of a uniform intensity beam that would produce threshold damage for a given pulse width, τ. However, since Q_c and T_c are not known, we have elected to determine whether reasonable values for them could lead to predicted values of thermal flux and pulse width that agree with the measured values of F_0 and τ at the damage threshold. Another difficulty in applying this model is that the experiments are conducted with a laser beam having a Gaussian intensity profile; therefore, the damage would occur first in a region centered on the beam axis, and the radial heat conduction would remove some energy from this region. In the absence of phase transitions, radial heat flow would cause the peak temperature to be lower than it would be if the beam were uniform, as implied by the results on beam diameter dependence discussed in the previous section (cf. Fig. 25). As a first approximation to incorporate the effect of radial heat flow into the uniform beam problem, we replace the actual Gaussian beam problem, in which the peak irradiance is I_0, with a uniform beam problem having an effective heat flux, F_0. The value of F_0 is chosen such that, in the

[26]F. Bartoli, M. Kruer, L. Esterowitz, and R. Allen, "Laser Damage in Triglycine Sulfate: Experimental Results and Thermal Analysis," *J. Appl. Phys.* **44**, 3713-3720 (1973).
[27]F. Bartoli, L. Esterowitz, M. Kruer, and R. Allen, "Thermal Modelling of Laser Damage in 8-14 μm Hg Cd Te Photoconductive and Pb Sn Te Photovoltaic Detectors," *J. Appl. Phys.* **46**, 4519-4525 (1975).

absence of a phase transition, the calculated peak temperature at the end of the exposure would be the same as it would be for the actual Gaussian beam. Having done this, the data points in Fig. 35 are the experimental values of the effective fluxes (adapted from Table 1) that produce threshold damage at the given pulse widths. The curve gives the theoretical predictions of Eq. 5 for a transition that occurs at a temperature increase of $33°C$ ($T_c = 68°C$), with $Q_c = 0.084$ J/cm^2. If a reasonable fraction of the epithelial material in the region of the wound (e.g., 5%) undergoes the phase change, then the value of Q_c would correspond to a latent heat of approximately 80 cal/g. These values of T_c and latent heat are both physically reasonable. Thus, in spite of the simplistic nature of this new model, these results suggest that endothermic phase transitions can explain the observed damage thresholds. Similar calculations should be performed for more realistic phase transition models that also account for the Gaussian irradiance profile and for multiple-pulse exposures.
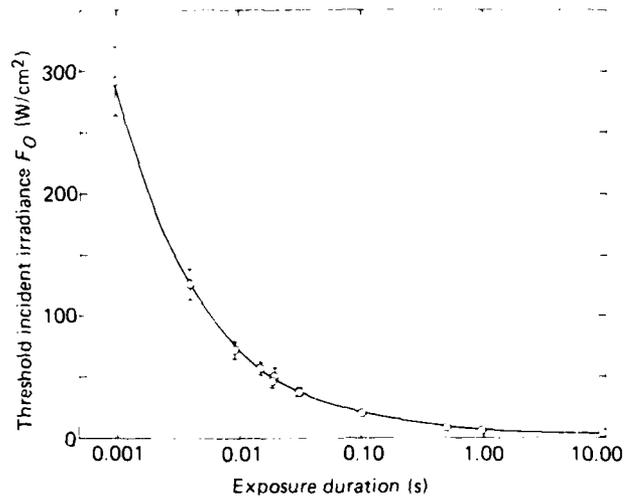
Figure 35 The data points are the experimental values of the effective flux, F_0 (adapted from Table 1), which produces threshold damage at the indicated single-pulse exposure duations. The ±10% error bars reflect both the bracket spacing in determining the threshold and the estimated accuracy of the power measurement. The curve is the theoretical prediction from Eq. 5 for the indicated parameters. The figure suggests that all of the single-pulse data can be explained by the model that incorporates a phase transition.

REFERENCES

[1] C. B. Bargeron, W. R. Green, R. A. Farrell, and R. L. McCally, "Structural Alterations in the Cornea from Exposure to Infrared Radiation," Annual Report to Letterman Army Institute of Research, Presidio of San Francisco, Calif. (Jul 1978).

[2] R. L. McCally, "Measurement of Gaussian Beam Parameters," *Appl. Opt.* **23**, 2227 (1984).

[3] A. S. Brownell and B. E. Stuck, "Ocular and Skin Hazards from CO_2 Laser Radiation," in *Proc. 9th Army Science Conf.*, pp. 123-138 (Jun 1974).

[4] D. E. Egbert and E. F. Maher, *Corneal Damage Thresholds for Infrared Laser Exposure: Experimental Data, Model Predictions, and Safety Standards*, U.S.A.F. School of Aerospace Medicine, Brooks AFB, SAM-TR-77-29 (1977).

[5] C. B. Bargeron, R. L. McCally, and R. A. Farrell, "Calculated and Measured Endothelial Temperature Histories of Excised Rabbit Corneas Exposed to Infrared Radiation," *Exp. Eye Res.* **32**, 241-250 (1981).

[6] C. B. Bargeron, R. A. Farrell, W. R. Green, and R. L. McCally, "Corneal Damage from Exposure to Infrared Radiation: Rabbit Endothelial Damage Thresholds," *Health Phys.* **40**, 855-862 (1981).

[7] H. S. Carslaw and J. C. Jaeger, *Conduction of Heat in Solids*, Oxford University Press, Oxford (1959).

[8] S. G. Bankoff, "Heat Conduction or Diffusion with Change of Phase," *Adv. Chem. Eng.* **5**, 51-122 (1964).

[9] C. B. Bargeron, R. A. Farrell, W. R. Green, and R. L. McCally, "Structural Alterations in the Cornea from Exposure to Infrared Radiation," Annual Report to Letterman Army Institute of Research, Presidio of San Francisco, Calif. (Sep 1979).

[10] H. Y. Ölcer, "On the Theory of Conductive Heat Transfer in Finite Regions with Boundary Conditions of the Second Kind," *Int. J. Heat Mass Transfer* **8**, 529-556 (1965).

[11] E. S. Beatrice and B. E. Stuck, "Ocular Effects of Laser Radiation: Cornea and Anterior Chamber," *AGARD Lecture Series Vol. 79, Laser Hazards and Safety in the Military Environment*, p. 5 (1975).

[12] D. L. Van Horn and R. A. Hyndirck, "Endothelial Wound Repair in Primate Cornea," *Exp. Eye Res.* **21**, 113-124 (1975).

[13] D. J. Spence and G. A. Peyman, "A New Technique for the Vital Staining of the Corneal Endothelium," *Invest. Ophthalmol.* **15**, 1000-1002 (1976).

[14] J. K. McEnerney and G. A. Peyman, "Indocyanine Green—A New Vital Stain for Use Before Penetrat-

ing Keratoplasty," *Arch. Ophthalmol.* **96**, 1445-1447 (1978).

[15] K. F. Palmer and D. Williams, "Optical Properties of Water in the Near Infrared," *J. Opt. Soc. Am.* **64**, 1107-1110 (1974).

[16] R. L. McCally, C. B. Bargeron, W. R. Green, and R. A. Farrell, "Stromal Damage in Rabbit Corneas Exposed to CO_2 Laser Radiation," *Exp. Eye Res.* **37**, 543-550 (1983).

[17] R. A. Farrell, R. L. McCally, C. B. Bargeron, and W. R. Green, "Alterations in the Cornea from Exposure to Infrared Radiation," Annual Report to Letterman Army Institute of Research, Presidio of San Francisco, Calif. (Sep 1982).

[18] N. A. Peppers, A. Vassiliadis, L. G. Dedrick, H. Chang, R. R. Peabody, H. Rose, and H. C. Zweng, "Cornea Damage Thresholds for CO_2 Laser Radiation," *Appl. Opt.* **8**, 377-381 (1969).

[19] R. A. Farrell, C. B. Bargeron, R. L. McCally, and W. R. Green, "Structural Alterations in the Cornea from Exposure to Infrared Radiation," Annual Report to Letterman Army Institute of Research, Presidio of San Francisco, Calif. (Jan 1985).

[20] R. L. McCally, C. B. Bargeron, W. R. Green, and R. A. Farrell, "Beam Diameter Dependence and Healing Processes in CO_2 Laser Damaged Corneas," Abs. Suppl., *Invest. Ophthalmol. Visual Sci.* **25**, 328 (1984).

[21] F. C. Henriques, Jr., "Studies of Thermal Injury V. The Predictability and the Significance of Thermally Induced Rate Processes Leading to Irreversible Epidermal Injury," *AMA Arch. Pathol.* **43**, 489 (1947).

[22] M. L. Wolbarsht, "Laser Surgery: CO_2 or HF," *IEEE J. Quantum Electron.* **QE-20**, 1427-1432 (1984).

[23] P. M. Morse and H. Feshbach, *Methods of Theoretical Physics*, McGraw-Hill, New York (1953).

[24] B. E. Stuck, D. J. Lund, and E. S. Beatrice, *Repetitive Pulse Laser Data and Permissible Exposure Limits*, Institute Report No. 58, Letterman Army Institute of Research, Presidio of San Francisco, Calif. (Apr 1978).

[25] D. J. Lund, B. E. Stuck, and E. S. Beatrice, *Biological Research in Support of Project MILES*, Institute Report No. 96, Letterman Army Institute of Research, Presidio of San Francisco, Calif. (Jul 1981).

[26] F. Bartoli, M. Kruer, L. Esterowitz, and R. Allen, "Laser Damage in Triglycine Sulfate: Experimental

Results and Thermal Analysis," *J. Appl. Phys.* **44**, 3713-3720 (1973).

[27]F. Bartoli, L. Esterowitz, M. Kruer, and R. Allen, "Thermal Modelling of Laser Damage in 8-14 μm Hg Cd Te Photoconductive and Pb Sn Te Photovoltaic Detectors," *J. Appl. Phys.* **46**, 4519-4525 (1975).

BIBLIOGRAPHY OF PUBLICATIONS
PREPARED UNDER CONTRACT

Papers:

C. B. Bargeron, R. L. McCally, and R. A. Farrell, "Calculated and Measured Endothelial Temperature Histories of Excised Rabbit Corneas Exposed to Infrared Radiation," *Exp. Eye Res.* **32**, 241-250 (1981).

C. B. Bargeron, R. A. Farrell, W. R. Green, and R. L. McCally, "Corneal Damage from Exposure to IR Radiation: Rabbit Endothelial Damage Thresholds," *Health Phys.* **40**, 855-862 (1981).

R. L. McCally, C. B. Bargeron, and R. A. Farrell, "Stromal Damage in Rabbit Corneas Exposed to CO_2-Laser Radiation," *Exp. Eye Res.* **37**, 543-550 (1983).

R. A. Farrell, C. B. Bargeron, W. R. Green, and R. L. McCally, "Collaborative Biomedical Research on Corneal Structure," *APL Tech. Dig.* **4**, 65-79 (1983).

R. L. McCally, "Measurement of Gaussian Beam Parameters," *Appl. Opt.* **23**, 2227 (1984).

Abstracts:

R. A. Farrell, R. L. McCally, and C. B. Bargeron, "Corneal Damage from Exposure to Infrared Radiation: Calculated and Measured Endothelial Temperature Histories," Abs. Suppl., *Invest. Ophthalmol.*, 106 (Apr 1979).

C. B. Bargeron, R. L. McCally, and R. A. Farrell, "CO_2-Laser Damage Thresholds in the Cornea: A Critical Temperature vs a Damage Integral Mechanism," 4th International Congress of Eye Research, New York, New York, (Sep 28-Oct 3, 1980).

C. B. Bargeron, R. L. McCally, W. R. Green, and R. A. Farrell, "Stromal Damage from Corneal Exposure to Infrared Radiation," Abs. Suppl., *Invest. Ophthalmol.* **22**, 30 (1982).

R. A. Farrell, R. L. McCally, and C. B. Bargeron, "CO_2-Laser Damage Thresholds in Rabbit Corneal Epithelium: Deviations from a Simple Critical Temperature Model," Abs. Suppl., *Invest. Ophthalmol.* **24**, 121 (1983).

R. L. McCally, C. B. Bargeron, W. R. Green, and R. A. Farrell, "Beam Diameter Dependence and Healing Processes in CO_2-Laser Damaged Corneas," Abs. Suppl., *Invest. Ophthalmol.* **25**, 328 (1984).

INITIAL DISTRIBUTION EXTERNAL TO THE APPLIED PHYSICS LABORATORY*

ORGANIZATION	LOCATION	ATTENTION	No. of Copies
DEPARTMENT OF THE NAVY			
NAVPRO	Laurel, MD		1
NAVSEASYSCOM	Washington, DC	SEA-9961	2
NAVAIRSYSCOM	Washington, DC	AIR-7226	2
DEPARTMENT OF THE ARMY			
Letterman Army Institute of Research	Presidio of San Francisco, CA	SGRD-ULZ-RC/R. McHenry	100

Initial distribution of this document within the Applied Physics Laboratory has been made in accordance with a list on file in the APL Technical Publications Group.